Published in final edited form as:
Cytometry B Clin Cytom. 2009 September ; 76(5): 295–314. doi:10.1002/cyto.b.20480.

Advances in Complex Multiparameter Flow Cytometry Technology: Applications in Stem Cell Research

Frederic Preffer[*] and **David Dombkowski**
Massachusetts General Hospital, Department of Pathology

Abstract

Flow cytometry and cell sorting are critical tools in stem cell research. Recent advances in flow cytometric hardware, reagents and software have synergized to permit the stem cell biologist to more fully identify and isolate rare cells based on their immunofluorescent and light scatter characteristics. Some of these improvements include physically smaller air-cooled lasers, new designs in optics, new fluorescent conjugate-excitation pairs, and improved software to visualize data, all which combine to open up new horizons in the study of stem cells, by enhancing the resolution and specificity of inquiry. In this review, these recent improvements in technology will be outlined and important cell surface and functional antigenic markers useful for the study of stem cells described.

Introduction

Stem Cells, Applied Therapeutics and Flow Cytometry

Stem cells are characteristically defined as quiescent, multipotent cells with the capacity for asymmetric self renewal and differentiation (1,2). The self-renewing capacity of stem cells ensures the integrity of the various anatomic compartments of the host, throughout its lifetime. Stem cells have been isolated from numerous anatomic locations and are most often classified based on the tissue from which they have been purified, and on the types of cells into which they differentiate. When isolated from their natural milieu and placed within in vitro culture, stem cells tend to differentiate into mature cells belonging to the tissue of origin. Their potential in regenerative medicine relies on the understanding of how they interact with their microenvironment or stem cell niche (3). This protective environment contains a variety of differentiated cells that secrete factors and fosters an environment that permit stem cells to both self-renew and/or differentiate along either multiple or individual lineages.

Over the last decade there has been extraordinary growth in stem cell research and related applied clinical practices. This has largely followed on the heels of the increasing success of bone marrow transplantation for the therapeutic treatment of malignancies, as well as continued progress in solid organ transplantation. Bone marrow transplantation has demonstrated that stem cell transplantation can have a palpable impact on improved therapeutic outcomes, and can even be combined with solid organ transplantation for improved outcomes (4). Complications with long-term immunosuppressive drug therapy, chronic rejection and the need for greater numbers of solid organs for transplantation than available have prompted the emerging field of regenerative medicine.

[*]Correspondence to: F. Preffer, PhD, Massachusetts General Hospital, 185 Cambridge Street, CPZN Room 4-226, Boston, MA 02114. E-mail: preffer@helix.mgh.harvard.edu.

Equally critical when postulating stem cell transplantation is the immunological safety associated with the graft. Transplanted stem cell grafts are potentially tumorigenic or infectious, and must be implanted and tolerated without rejection by the host, or in the case of hematological grafts, graft versus host disease (GVHD). The theoretical prospect of possibly transplanting MHC deficient cells must be weighed against both their being prime targets of host NK lysis and the reality that many lethal human malignancies are those which have poor MHC expression and thus escape host recognition.

Thus, the study of stem cell biology offers the biologist the opportunity to study the mechanisms that regulate embryonic and cellular differentiation and tissue maintenance, and to clarify the molecular and immunological mechanisms underlying this establishment. Based on the premise of more fully understanding these processes, there is great potential for enhancing present stem-cell based therapies and developing new ones directed against degenerative diseases. By extension, with a further understanding of the dysregulation of stem cell differentiation, it might be possible to gain better perspective into the causes of the malignant transformation of cells (5). Aiding all of these endeavors has been the technology of flow cytometry and cell sorting, which continues to play a pivotal role in enhancing our understanding of these cellular processes.

Flow cytometry offers the ability to examine rapidly thousands of cells stained with monoclonal antibodies conjugated to fluorescent dyes. Each cell is individually assessed for a variety of characteristics such as size and biochemical and/or antigenic composition. High precision and sensitivity, combined with the large numbers of cells that can be examined permits resolution of even very minor subpopulations from complex mixtures with high levels of statistical validity. The capacity to physically separate these subpopulations by flow sorting allows further functional, morphological and molecular correlations to be determined.

Since the inception of flow cytometry and fluorescence activated cell sorting in the mid to late nineteen sixties (6,7,8,9,10) the technology, coordinated with progress in monoclonal antibody production, has become incorporated into fields encompassing predominantly human clinical medicine and biomedical research. This has primarily been in areas of immunology, pathology, oncology and molecular biology, such as the diagnosis of hematopoietic malignancies and monitoring of HIV/AIDS and other research areas related to cell signaling, viability and apoptosis. However, cytometry has additionally found use in veterinary medicine, agricultural, oceanic and even astronomical research. It is widely accepted that the technology has provided a critical impetus to modern immunology and proteomics and is a cornerstone of current stem cell research. Just as each of the aforementioned disciplines requires modifications and specific alterations of the basic technology, the use of cytometry in stem cell research also has unique requirements. Numerous reviews and books are available to begin to learn about the technology related to flow cytometry and cell sorting (11,12,13,14,15,16,17). In this review, we will delegate these available reviews and books to update the reader on ‘the basics’ of cytometry and concentrate on relatively newer technologies related to instrument design and advances in reagents and analytic software. There will also be an overview of important cell surface antigens and functional markers that are available for flow cytometry that have been useful for stem cell research.

While routine ~4-color flow cytometric analysis has been effectively utilized for research and clinical analysis for many years, recently our laboratory and others have been exploring the potential of greater immunofluorescent capacity for stem cell research. With new concept instruments, reagents and software similar to that described below, we aspire to take this capacity to yet a higher level. While these technologies are presently in their nascent

stages, advances in research have been forthcoming (15,18,19,20) forecasting their practical utility in stem cell research, with eventual emergence into the clinical diagnostic setting (21). The use of polychromatic (>5 colors) cytometry has been made possible by advances in three technically interrelated areas:

1] Introduction and general commercial availability of appropriately configured cytometric hardware with multiple excitation sources, highly sensitive collection optics and digital electronics—High quality multilaser platform instruments started becoming commercially available beginning around 2002. These instruments contained air-cooled diode-pumped solid state and laser diodes, high efficiency optics, electronics and fluidics which all combined to both improve the resolution and efficiency and reduce the cost of high quality analyzers. For example, prior to these key advances, the requirement for high-power ultra-violet ion-laser sources, and their related expensive infrastructural support inhibited the study of side population (SP) cells and other assays requiring ultra- or near violet excitation (22,23). This successful platform design combination also forecast similar advances in cell sorter assembly, permitting smaller footprint cell sorters that were as capable or in some ways even superior to their physically larger predecessors. For example, in some designs, utilization of flexible fiber optics to route signals from the flow cell to PMT arrays provided overall greater design adaptability.

2] Increased commercial availability of monoclonal antibodies directed to leukocyte differentiation antigens conjugated to fluorochromes with excitation maxima proximal to multiple available excitation sources—Until recently it was extremely difficult to obtain monoclonal antibodies conjugated with anything other than 488nm and 632nm –excited fluorchromes from commercial sources; fortunately the availability of other fluorochromes conjugated to antibodies have expanded significantly in the last few years. Fluorochromes chosen should have high extinction coefficients and quantum yields, be easily conjugated to monoclonal antibodies and have little spectral overlap with other conjugates. Beginning at the ‘most violet’ end of the spectrum, the UV-excitable Alexa 350 and AMCA-X fluorochromes can be conjugated to monoclonal antibodies, and serve as potential labels. Although not useful for antibody labeling, but helpful since the inception of flow cytometry, Hoechst 33342 is required for side-population studies (24,25) and 4′, 6-Diamidino-2-phenylindole dihydrochloride (DAPI) is useful for cell cycle and/or DNA-ploidy studies. Useful conjugatable violet [~405nm] excitable dyes include AmCyan 403, Pacific Blue, Pacific Orange, Alexa 405, Alexa-430, V450 and a variety of quantum dots [e.g. Qdot™, eFluor™, AxiCad™ nanocrystals]. Quantum dots [semiconductor nanocrystals] did not initially easily conjugate to monoclonal antibodies and when unbound were prone to aggregation, but have recently improved in performance. Blue [~488nm] excitation is best for FITC, Cy3 and peridinin chlorophyll protein (PerCP). PerCP is similar in emission to the tandem PE-Cy5, with less red spillover than the tandem. However, PerCP conjugates are ‘bleached’ easily and thus cannot be used with the higher-power argon-ion lasers commonly found on stream-in-air cell sorters. Green [~532nm] or preferably yellow-green [~565nm] excitation lines are best for phycoerythrin (PE) excitation and red [~633nm] for allophycocyanin (APC) and both their respective tandem-conjugates of Cy5, Cy5.5 and Cy7. Tandem dyes, which rely on the resonance energy transfer between closely approximated donor and acceptor fluorochromes tend to have a propensity for non-specific binding, instability and lot-to-lot variation even when obtained from one source, and thus also must be used cautiously. Recently, HiLyte 750 has been shown to be useful when used as a tandem conjugate with APC since it is more stable to light exposure than Cy7, which significantly reduces spillover into the APC channel. Somewhat more esoteric, but useful conjugates of Alexa 594 and LI-COR IR-Dye 800CW can be used with yellow and infra-red lasers, respectively (Figure 1). Very low background fluorescence in the IR range

provides for a much higher signal-to-noise ratio than visible fluorophores, which helps compensate for the relatively lower photon counting statistics in the far-red region. In the future, the use of avalanche photo-diodes to capture these far-red emissions may prove to be superior to anything but the most red-sensitive PMTs (26).

3] Operational and analytic software capable of functioning in the digital domain, permitting the numerous required intra- and inter- laser fluorochrome compensation calculations—Due to the complexity of compensating polychromatic fluorescent signals it is essential to rely on software-based matrixes that can objectively adjust the compensation settings after the data is collected and apply bi-exponential scaling (27). While software has matured well enough to tackle this particular need, currently available analytic software is still relatively primitive in fully exploiting the potential of polychromatic analysis, with respect to 'data-mining.' That is, although the software is functional, it is suboptimal in that compared to 3–4 color analysis, most existing software platforms scale poorly when larger polychromatic data-sets require processing; 'data-mining' then becomes a very time consuming process. Furthermore, the voluminous number of bivariate plots resulting from the analysis of a polychromatic data set tends to inhibit rather than help inquiry. Additionally, "gating" remains a relative subjective process with the potential loss of data, especially when numerous gates are applied.

While the convergence of the aforementioned improvements in hardware, reagents and software permit our present capacity, the techniques to reproducibly stain cells with ≥10–12 directly conjugated fluorochromes is presently at a relatively early stage. Although the initial step of consulting a table of dye excitation and emission maxima and matching these to band-pass filters and excitation sources is necessary, it is insufficient to attain reliable polychromatic capacity without equal and strict attention to issues related to reagent titration, potential dye-dye interactions, fluorescence compensation and staining controls (15,17,28). Our initial results years ago using stream-in-air cell sorters were initially disappointing when attempting resolution of ~7 markers; however, after access to the light collection improvements inherent in cuvette-design technology, many of the problems were quickly surmounted. For example, the increased optical efficiency inherent in a gel-to-objective-coupled cuvette over cell interrogation through a 'lens-like' stream-in-air sorter provided a superior signal. While the need for controls and compensation matrices presently require more care than routine 4-color work, these obstacles have been reasonably surmounted, as indicated, with improved software. Cumulative and incremental improvements in achieving maximal signal-to-noise ratios for each fluorochrome, such as optimized optical filter selection and refining detector voltages were additionally helpful. Increased awareness of fluorescence detector performance and tools with the capacity for measuring and tracking cytometer resolution [Q =efficiency, and B= background] also serve to improve the quality and reproducibility of instrumental measurement (29,30).

Table 1 indicates the excitation and emission characteristics of some of the fluorescent conjugates and probes and commonly used excitation lines we find useful:

New Technology- Multi-Laser Cytometers: Access to cytometers with more than two-three lasers is becoming common place

Recently, our laboratory has constructed a unique prototypic 7-laser instrument (Becton Dickinson, San Jose CA). The instrument is both stable and highly configurable, which is valuable in a varied research setting where flexibility in excitation source wavelength plays a critical role. This instrument permits us to fully exploit new reagent combinations and seek laser/dye combinations with minimal compensation between fluorochromes. The new concept is to improve measurements (photon counting statistics) by combining increased

laser powers (e.g. up to 100 mW at 488 nm) and multiple laser excitation line flexibility with enhanced optical collection efficiency to minimize measurement error and improve resolution of relevant biological populations. Furthermore, to increase flexibility, optical switchboxes can redirect the emission light paths between different fluorescence collection optics configurations containing either 8 (octagon) or 3 (trigon) PMT channels.

The instrument is configured with the following lasers and PMT arrays, arranged as depicted in Figure 2:

This instrument's design permits choice of selected antibody-fluorochrome combinations that require minimal compensation, in part by permitting a theoretical reduction in the number of fluorochrome excitations per laser to ~2. That is, rather than simultaneously using every possible fluorochrome that the green laser can excite, we choose among conjugated probes spread throughout a wide excitation spectrum to minimize inter- and intra- laser compensation needs, increasing the resolving power of the instrument (Figure 3). The appropriate integrated use of these 7 excitation sources with suitable fluorochromes permit reduced spillover correction/compensations between all fluorescent parameters, in contrast to using relatively fewer excitation lines and more fluorochromes per line. A high efficiency quartz cuvette captures and directs seven temporal and spatially discrete signals via distinct fiber-optics to seven PMT populated arrays. The PMT-populated octagonal arrays provide the flexibility to use present antibody-fluorochrome conjugations as well as anticipated new fluorochromes in the future (31,32,33). New fluorochromes for immunophenotyping applications are consistently being developed, such as violet excitation of quantum dots conjugated to monoclonal antibodies (34,35,36) eFluor crystals, UV (AMCA-x) and infrared (IRDye 800CW) dyes. Further flexibility in excitation sources might be obtained in the near future with a new family of rare-earth [Tm^{3+} and Yb^{3+}] 'up-converted' nanophosphors which will open up the infrared region to flow and image cytometry (37).

Cytometric Data Representation: Present Software Limitations and Solutions

Presently, flow cytometry data is most commonly depicted on two dimensional "x versus y" Cartesian dot- or contour -plots, with a possible third dimension in the z-plane identified with color as a sign of density or relationship to a gated parameter(s). The goal of any and all analytic software should be to aid the researcher by providing the most concise data for either cell sorting or analysis. There are a variety of commercial approaches to this from the numerous instrument manufacturers [e.g. Accuri, Beckman Coulter, Becton Dickinson, Guava, Partec. Additionally, 'third party" approaches to data analysis are available from De Novo, Tree Star, VenturiOne™, and Verity Software, as well as numerous open source products [e.g. WinMDI, IDLYK, ANALYSE and LAP].

Multiparameter or polychromatic populations require complex Boolean gates or multiple, hierarchical gates to resolve desired subpopulations. The logarithmic axes generally extend over a four to five decade range, representing cells with 10- to 100- thousand fold intensity disparities between the least and most expressive cells. These plots are easy to inspect and enjoy wide acceptance by the scientific community. While such data representation is acceptable and sufficient for inspection of ~ 4–5 multiparameter fluorescent parameters, the number of bivariate plots quickly increase to an unwieldy number with polychromatic data; the total number of bivariate plots needed to project P parameters is $P \times (P-1)/2$. For example, use of 4 immunofluorescent parameters results in 6 bivariate plots to examine; however if 17 markers are used there are 136 bivariate plots to inspect. This makes total comprehension of such information very difficult and inhibits an overall understanding of the data, due to the voluminous number of histograms requiring inspection. To attempt to break from the 'Cartesian handcuffs' of multiple bivariate plots, totally new ways of representing the data output of flow cytometers are emerging, incorporating alternative

approaches such as mixture modeling (38), cytometric fingerprinting (39), statistical manifolds (40) probability binning (41) use of heat maps and FCOM™-like additions (42). A further expanded repertoire of software tools are also emerging such as:

The **parallel coordinate plotting system** which is a graphical device for displaying data in high-dimensional space above three dimensions, and is also an alternative to the conventional scatter plot. Since plotting more than 3 orthogonal axes is difficult to represent in 2 dimensions, parallel coordinate schemes represent each parameter as a discreet axis and plot all the axes parallel to each other in a plane. In these plots, orthogonal axes are replaced by drawing the uniformly spaced axes parallel to each other such that each cytometric parameter has a unique representation. This results in improved 'scalability' compared to traditional bivariate dot-plots, resulting in a relatively compact two-dimensional visualization of the polychromatic data set (43,44). To address some of the problems with visualizing huge data sets, the two-dimensional data can be clarified by adding an iso-surface in the z-dimension denoting the density of events or as a 'gating' tool analogous to that used in Cartesian dot-plots (45) or by utilizing feature animation or high precision textures (46). This approach is being developed in our laboratory as an exciting and helpful new way of addressing the need for an improved method of inspecting large polychromatic data sets, as shown in Figure 4.

Another novel presentation tool is the **polyvariate display** function (FlowJo;Tree Star, Inc.) which is another way to display more than 2 parameters on a 2D graph, permitting the user to define complex populations of cells using one gate. This tool uses a vector control and pivot range integrated with the polyvariate plot whereby the origin is the center of a circle; the origin is the minimum value and the circumference is the maximum value. The vector angle determines the direction away from the origin the parameter will be scaled as shown in Figure 5.

A third novel approach currently under development incorporates a **probability state model** (Gemstone; Verity Software). This is a new concept which avoids the pitfalls of numerous bivariate plots in favor of a newly conceived scalable display tool. The software avoids gating problems by defining overlapping populations probabilistically (47). The model defines a 'state index' which is an additional parameter based on states and probabilities. This parameter is used to correlate all the other parameters in the system and results in the ability to analyze multiple samples in a compact and comprehensible format (Figure 6). With a properly configured antibody –fluorochrome design, the software will also permit additive/concatenated staining so that common elements between staining tubes will serve as a scaffold to permit unique correlations between tubes to be viewed. The software can potentially serve as a sorting interface, making use of its unique analytical capacity to more easily and expeditiously identify complex immunophenotypes.

Promising Cell Sorting Technologies with an impact on applied stem cell research

Although high-speed hydrodynamically focused stream-in-air cell sorting is presently the gold-standard cell separation technology, there are numerous reasons why it is an impractical way to select large numbers of stem cells for potential large scale therapeutic use. Firstly, because conventional droplet sorters inspect cells serially they are intrinsically too slow to isolate large numbers of cells and their use risks both sample contamination and operator exposure to potentially hazardous material. One approach to enhance the speed of analysis is to increase the number of droplet sorters operating in parallel on the experimental sample, exemplified by the approach of the iCyt™ Reflection, which scales up to four sorting heads per instrument. Another prospective improvement would utilize a laser rastering system, in which an excitation beam of reduced width is rastered across the core stream, capturing cells from every portion of the stream. The design insures that every cell

would be repeatedly scanned to both limit cellular coincidence and increase performance throughput over conventional systems by five fold (48).

Rather than using sheath fluid to hydrodynamically focus cells, it is possible to focus and concentrate them using acoustic excitation. There are practical advantages to omitting sheath fluid including significant cost and instrument-size savings, in addition to the ability to repeatedly reanalyze cells for reliable rare event analysis (49).

In contrast to droplet sorting, the micro-fluidic switch sorting technology does not require droplet formation and can take place within an entirely enclosed sterile and disposable fluidic path. However, micro-fluidic switch sorting has been relatively slow (~ 200 cells/second) compared to conventional high-speed droplet sorters operating at an upper range of ~25–35,000 cells/second (50).

Two important recent developments have dramatically increased the overall cell sort rate in micro-fluidic switch sorting. These are a 10-fold increase in sort rate and parallel implementation of multiple switches on a single disposable chip. The disposable chip is embedded in a single-use, disposable cartridge that contains the entire fluid system of the flow sorter (51). This emerging technology (e.g. the Gigasort™ from Cytonome) overcomes the limitations in switch-sorting cell processing speed, selection capability and cGMP compliance and will enable sample throughput rates of up to 1×10^9 cells per hour (~280,000 cells/second). It is likely that future cell separation techniques will capitalize on further advances in microfabrication which will serve to both shrink the size and cost of instrumentation, while vastly increasing their scalability and capability up to 32 fluorescent parameters (52), resulting in high-throughput ‘lab-on-a-chip’ instruments (53,54).

While stream-in-air sorting remains the gold standard for rapidly separating cells in suspension, it is of more limited utility for small numbers of adherent, biohazardous and/or fragile cells. Other issues related to both altered gene expression and physiology related to detaching adherent cells can also limit the utility of cell sorting. Thus, it is worthwhile to mention laser-enabled analysis and processing (LEAP™) technology, which can image and purify adherent cells by a variety of laser-mediated cell manipulations in a high-throughput fashion (55).

Although not a cell separation technology, it is worth noting that the combination of flow cytometry and quantitative cell imaging has been accomplished in the Amnis ImageStream™ system. This technology has recently improved its capacity to visualize cells with an enhanced depth-of-field technology and has been involved in advancing stem cell research in areas related to Wnt signaling (56), leukemic stem cells (57), pluripotent stem cells (58) as well as helping define ‘very small embryonic-like stem cells’ (59).

II. Antigenic and Functional Markers Useful for the Study of Stem Cells

Stem cells are characteristically identified by cell surface or functional markers, or combinations of the two, by flow cytometry. Since stem cells are profoundly scarce, when attempting to analyze or physically separate them based upon multiparametric characteristics it is extremely useful to physically remove fully differentiated cells with ‘mature’ cell markers. For example, in separating hematopoietic stem cells from human bone marrow, cord or peripheral blood, it is often best to initially apply biotinylated conjugated cocktails of CD45, CD3, CD4, CD8, CD19, CD56, CD16, CD14, CD33, CD11b, CD61, and CD71. In the mouse, analogous markers including B220, Mac-1, Gr-1, CD4, CD8 and Ter119 are best utilized (60). These labeled cells are then removed by parallel ‘negative selection’ sorting with streptavadin conjugated paramagnetic beads in a strong magnetic field, resulting in a lineage negative (Lin−) population that can be subsequently

labeled for serial 'positive' selection or identification by flow cytometry. Various manual and automated systems are commercially available for this step (e.g. Miltenyi, Dynal, Robosep, IMag). The benefit of this procedure is that cells otherwise present at 'fractions of a percent' can be more effectively positively identified and/or sorted with increased levels of purity and recovery. A pitfall is that extremely rare cells may be nonspecifically "trapped" by numerous differentiated cells during the magnetic bead sort. When desired rare subpopulations are relatively better represented, rather than their physically separation, Lin+ cells can be relegated into a fluorescent 'dump channel,' in which all Lin+ cells are stained with the identical fluorochrome. Then, antigenic co-expressions are more easily visualized on rare cells without impediment by differentiated cells. Some of the technological advances in the previous section, such as the increased analytical sensitivity and precision afforded by the use of multiple higher power solid state lasers, become extremely useful in obtaining this information.

A complete review of stem cell immunophenotyping is beyond the scope of this review; however, as an aid to those relatively new to the field, Table 2 illustrates some antigens which have primarily been useful in the study of human and murine hematopoietic and other stem or progenitor cells. Following the table are further specifics in an 'antigenic approach' to these and other functional markers, in some cases including murine studies which were helpful in the development and further understanding of progenitor, stem and cancer stem cells.

Lineage negative, cKit+, SCA−1+ (LKS)

Initially, hematopoietic stem cells (HSC) were defined in the murine system by the combination of the absence of mature lineage antigens CD4, CD8, Ter119, Gr-1, Mac-1 (Lin^{neg}), the presence of stem cell antigen expression (SCA-1+) and reduced expression of the Thy-1 ($Thy\text{-}1^{lo}$) marker (61,62,63). This initial approach was subsequently modified with the use of the tyrosine kinase receptor CD117 (c-Kit), CD34 negativity, the membrane glycoprotein CD135 (Flt3) and CD150 expression to help distinguish hematopoietic stem cells (Lin^{neg} - c-Kit+ SCA-1+, $Thy1.1^{lo}$, CD34-, Flt3−, CD150+, CD244−) from multipotent progenitors (Lin^{neg} c-Kit+ SCA-1+, $Thy1.1^{lo}$, CD34+, Flt3+, CD150− CD244+ ; 64,65,66). It remains that these marker combinations are very useful, but likely describe overlapping populations, especially when dye efflux capacity {vide infra} is added as a functional parameter. Thus, it is prudent to recognize that there is presently no standard in distinguishing stem from progenitor cell populations especially when strain, animal developmental age and potential mutant mouse models are considered. For example, Thy1 expression is only useful in strains carrying the allele, and selection based on CD34- requires the use of mice >8 weeks old. These complications are further compounded when considering the use of mutant murine strains, the technical staining competency and the type of cytometry equipment used.

CD34 is a stage-specific antigen that is expressed on human hematopoietic stem and progenitor cells whose expression decreases with differentiation of the cell. Human CD34 can be divided into three broad classes (I, II and III) of recognizable epitopes based upon their sensitivities to neuraminidase and the O-sialoglycoprotease from *P. haemolytica* (67). Selection of a properly titrated antibody and fluorochrome-conjugate is essential to obtain valid information since not all classes of antibody uniformly stain the antigen. For example, most Class I antibodies have lower avidities and are not recommended for use in immunodiagnostic panels. In contrast, PE-conjugates of Class III (e.g. clones 8G12, 581) and Class II (QBEnd10) detect identical populations. However, FITC conjugates of QBEnd10 do not have the same reactivity, likely due to inhibition by the negatively charged glycan target and the negative charge conferred to the antibody by the FITC conjugate (68).

CD34+ cells are heterogeneous and their co-expression of other markers such as CD38, CD123, HLA-DR, CDCD45RA, CD71, CD90, CD117, and Rhodamine123 have been used to distinguish subpopulations enriched in progenitor populations (69). For example, subsets of CD34+ CD109+ cells obtained from fetal and adult bone marrow have been shown to define pluripotent megakaryoblast and myelo-erythroid progenitors (70). Recently, human HSC obtained from cord blood have been identified as Lin^{neg} CD34+CD38−CD90+CD45RA− and were distinguished from Lin^{neg} CD34+CD38−CD90−CD45RA− multipotent progenitors using both xenotransplantation and in vitro assays (71).

Murine CD34 has been shown to have similar biochemical and functional properties with a similar cellular distribution as human CD34 (72). Although CD34 knockout mice contain reduced numbers of hematopoietic precursors the animals have normal bone marrow and peripheral blood counts, pointing to a redundancy in CD34 function with some other cell type (73).

SLAM—While the Lin^{neg} c-kit+ Sca-1+ Thy^{lo} markers have been the defacto standard for murine stem cell isolation, the aforementioned problems regarding the complexity of their use as well as the sheer number of antibodies necessary presents an impediment to researchers, particularly for tissue based studies. The signaling lymphocyte activation molecule (SLAM) family of markers represents another resource for studying stem cells by flow cytometry. Reduced numbers of these markers in ‘coded’ combinations were reported to distinguish hematopoietic stem cells (SLAMf1/CD150+ CD244− CD48−) from multipotent (CD150− CD244+ CD48−) and B cell (CD150− CD244+ CD48+) progenitors. Moreover, the code of SLAM expression was found to be conserved among different and older mouse strains even if transplanted (74,75). Like many of the aforementioned markers described, there is likely significant overlap between these and other putative surface and functional stem cell markers.

CD133—(AC133 or Prominin-1) is a surface molecule expressed on primitive human progenitor cells of hematopoietic, endothelial, and neural epithelial lineages (76,77,78). CD133 is a 5-membrane–spanning cell surface molecule that does not share homology with previously described HSC surface antigens and is rapidly down-regulated as human HSCs differentiate into phenotypically restricted cells (79). Compared to CD34+CD133−cells obtained from cord blood, CD34+CD133+ cells were found to have much increased clonogenic and repopulating capacity when injected into NOD/SCID mice, and had seven-fold enrichment in functional dendritic cell precursors (69) and LTC-IC function. CD34+ CD133+ cells preferentially gave rise to granulocyte-macrophage colonies while CD34+CD133− cells produced erythroid colonies (80). Because cultured CD34−CD133+ cells isolated from cord blood have the capacity to generate CD34+ cells, it is hypothesized that the CD34−CD133+ immunophenotype might be ancestral to the CD34+ subpopulation (81). When peripheral blood CD133+ cells were cultured on fibronectin coated dishes in the presence of vascular endothelial growth factor, endothelial cells resulted from cells that initially expressed CD31+ (82). Neurons, astrocytes and rare oligodendrocytes resulted from adult and fetal human skin derived CD133+ cells, which also demonstrated self-renewing capacity. These cells, which co-expressed CD34+ and CD90+, were grown in medium containing epidermal and fibroblast growth factors and could implant and differentiate in adult mouse forebrain. Although unproven, it is possible that these skin derived CD133+ cells were derived from the blood (83). Another molecule found on normal and malignant hematopoietic CD133+ and CD34+ cells obtained from bone marrow, cord or peripheral blood is CD318 (CUB-domain-containing protein 1, or CDCP1). Interestingly, this antigen is also detected on mesenchymal and neural progenitor cells, suggesting it’s possible role as a multipotent adult progenitor cell marker (84).

CD117 also known as c-kit, steel factor, or stem cell factor (SCF) receptor/ligand is a proto-oncogene encoding a 145 kd tyrosyne kinase transmembrane receptor which plays a key role in haemopoiesis and belongs to the same family of receptors as platelet-derived growth factor and colony-stimulating factor-1 (85). In human bone marrow and cord blood CD117 is expressed on early myeloid progenitors and is down-regulated upon maturation, except on mast cells. Due to this characteristic expression, CD117 is especially useful in the differential diagnosis of acute myelogenous leukemia from acute lymphoblastic leukemia in the clinical flow cytometry laboratory. CD117 was first identified as the cellular homolog of the feline sarcoma viral oncogene v-kit (86).

The binding of SCF, which is produced primarily by marrow stromal cells to CD117 (87) leads to the dimerization of c-kit proteins, which initiates a signaling cascade that ultimately induces cell growth (86). CD117 is thus suggested to be involved in signaling, activation, and proliferation of cells and is found on a diverse group of histologically normal non-lymphoid cell types, such as breast epithelial cells, renal tubule cells, astrocytes, Purkinje cells, and endometrial cells (88).

Mutations in CD117 have been found to play a role in oncogenesis in a large number of neoplastic disorders such as systemic mastocytosis, gastro-intestinal stromal tumors (GISTs), germ cell tumors and acute myelogenous leukemia (89). Recent therapies (imatinib mesylate, or Gleevec) inhibiting specific mutations in the tyrosine kinases such as Bcr-Abel and the platelet derived growth factor receptor have been shown to be effective in treating malignancies that over-express this receptor such as chronic myeloid leukemia (90). This drug is also effective in therapies associated with CD117 expressing GISTs (89,91).

CD90 or **Thy-1** is a 25–37 kDa N-glycosylated, glycophosphatidylinositol anchored highly conserved cell surface protein, originally discovered as a rodent thymocyte antigen with a possible role in cellular activation. In mice it serves as a hematopoietic stem cell, pan-T, thymocyte, fibroblast and neural cell marker. In humans, Thy-1 expression appears more restricted, and is found on a small population of cortical thymocytes neurons and hepatic stem cells (92,93).

CD105—CD105 is a 180 kDa homodimeric transmembrane glycoprotein expressed predominantly on the cell surface of human endothelial cells and is thought to play an important role both in angiogenesis and hematopoiesis (94). The normal function of CD105 is associated with that of the transforming growth factor (TGF)-β receptor and is seen to significantly up-regulate on vascular endothelium in areas of inflammation and tumor growth (95). For human stem cell research, the combination of CD105+, CD73+, CD16+, CD90+ CD29+ CD34−, CD45−, CD14− has been useful in the purification of mesenchymal stem cells (MSC). MSC have the capacity to differentiate into bone, cartilage and fat and have been shown to have significant suppressive effects on the immune system of an allogeneic transplanted host, such as reversing GVHD (96). The mechanism of this immunosuppressive effect has been specifically related to altered cytokine secretion and concomitant reduction in inflammatory mediators within subsets of dendritic, T and NK cells (97).

CD135—FMS-like kinase-3 (FLT3) or STK-1, or Flk-2 is a member of the receptor tyrosine kinase type III family that also includes c-kit, c-FMS, and PDGFα/β. CD135 is a growth factor receptor and signaling through it plays a role in cell survival, proliferation, and differentiation. FLT3 expression in human bone marrow is restricted to CD34+ cells and a subset of dendritic precursors. CD135 is a proto-oncogene and internal tandem mutations of FLT3 play an important role in leukemogenesis; such mutations are associated with poor prognosis in acute myeloid leukemia (98).

In the murine system, the loss of CD90/Thy1 and gain of CD135/Flk2 expression marks the loss of self-renewal in HSC maturation. CD135 is expressed in short-term -HSCs but not long term –HSCs (99).

Functional Stem Cell Markers

Aldefluor is a non-immunological reagent that has been used to identify human stem and progenitors in the bone marrow, mobilized peripheral and cord blood on the basis of the cytosolic aldehyde dehydrogenase (ALDH) activity in these cells. ALDH is found in primitive hematopoietic cells and converts the non-polar, membrane-diffusible substrate (bodipy- amino-acetaldehyde) into a negatively charged non-diffusible fluorescent bodipy-aminoacetate. ALDH serves as a 'de-toxifying' agent and confers stem cell resistance to alkylating agents such as cyclophoshphamide (100) as well as oxidizing vitamin A and ethanol (101). Additionally, since the polarized moiety can only be retained by cells with a patent cytoplasmic membrane, only viable cells are pinpointed. Similar to Hoechst exclusion, use of this reagent opens up a strategy of stem cell isolation based upon a relatively conserved stem cell function rather than an immunophenotype.

$ALDH^{bright+}$ Lin^{neg} cells have been shown to include an enriched expression of CD34+CD38−, CD133+ CD31+ and CD117+ (102) cells suggesting the presence of both hematopoietic and endothelial progenitors. These include functional populations capable of becoming colony forming cells, long-term culture initiating cells and NOD/SCID repopulating cells.

Relatively distinct hematopoietic compartments have been defined by use of aldefluor as a marker for ALDH activity with CD34+ umbilical cord blood (UCB) cells. Purified $ALDH^{bright+}$ CD34+ cells injected into NOD/SCID mice or placed in primary and secondary long-term culture were highly enriched for cells giving rise to multilineage development. In contrast, $ALDH^{-}$CD34+ or $ALDH^{bright+}$CD34− cells contained few progenitors (103).

Similar studies using ALDH $^{bright+}$ CD133+ Lin^{neg} cells obtained from UCB seeded the murine BM microenvironment within 48 hours after transplantation, expanded efficiently in vivo to produce mature myeloid and lymphoid progeny. These cells also continued to maintain a population with primitive hematopoietic phenotype, and consistently engrafted recipients of serial, secondary transplants, unlike their ALDH $^{bright+}$ CD133- Lin^{neg} counterparts (102).

Due to both the rarity of primordial neural stem cells (NSC) and absence of specific markers relative to those available in the hematopoietic system, ALDH activity has also been pursued in the study of neural stem cells. $ALDH^{bright+}$ SSC^{lo} cells obtained from murine embryonic forebrain germinal zones and adult forebrain subventricular zones were multi-potent and capable of self-renewal and generation of neurospheres and neuroepithelial cells. Upon transplantation into mouse brain, progeny of $ALDH^{bright+}$ cells differentiated into mature neurons detected in cortical and subcortical areas (104). Cells isolated from the caudal neural tube of embryonic rats were also found to express elevated levels of ALDH (105). $ALDH^{bright+}$ SSC^{lo} cells isolated from embryonic and adult spinal cord were also shown to be self-renewing and multipotent, and could restore partial function when transplanted intrathecally into a mouse model of spinal muscular atrophy (106).

Hoechst 33342—Hoechst 33342 is a live-cell permeant dye that binds into the minor grove of A-T rich regions of DNA (107). The dye is best excited by 350–360nm ultraviolet light and was initially useful in measuring cellular DNA content and proliferation in live-unfixed cells (108). Side population (SP) cells are stem and early progenitor cells identified as a subpopulation by their low Hoechst blue and red fluorescent emission signature. This is

evidenced as a trail of decreasing Hoechst fluorescence from a greater number of more differentiated cells, with increased fluorescence, that have loaded and retained the dye. When detecting SP cells, fluorescence is directed towards a 610nm dichroic and then captured simultaneously through both a 450nm band-pass and 675nm long-pass filter on a linearly amplified fluorescence scale. The characteristic Hoechst fluorescence SP 'tail' (Figure 7) is attributed to a highly active efflux of Hoechst 33342, via a p-glycoprotein multi-drug/ATP binding cassette transporter Bcrp/ABCG2 protein (24,109,110). The ATP transporter is otherwise thought normally responsible for biliary excretion, lipid translocation, and drug elimination.

The result of the high level of dye exclusion is that the fluorescence intensity of the nuclei in the resultant SP cell population is reduced relative to that in the nuclei of cells in the differentiated cell population. The presence of the pump is tested by its blockade with a specific metabolic inhibitor, such as verapamil or reserpine.

The SP staining protocol is relatively rigorous with dye concentration, incubation time and temperature relatively stringent; after staining, the cells must be maintained at 4°C prior to processing on the cytometers (107,111). It is very useful to include a viability dye (e.g. propidium iodide or 7-AAD) to discriminate dead from viable cells. Since the initial staining protocol was developed for isolating murine stem cells, the staining parameters might need to be optimized for other tissues or species (25,112).

Murine SP cells were initially defined by their relatively active efflux of Hoechst 33342, with the cells having the strongest dye efflux ability also having the highest hematopoietic repopulating capacity (113,114). Bone marrow derived SP cells were shown to be enriched 1000 fold for *in vivo* lymphoid and myeloid hematopoietic reconstituting activity. These earliest studies showed SP cells to be about 10% of the Sca-1+ $CD34^{-}$ murine BM, expressing CD117, CD43, and CD45 (113). Cell cycle analysis of SP cells revealed their relative quiescence; the few SP cells in growth phase [<2%] had repopulating capacity indistinguishable from those in $G_{O/1}$. More recently, cells with this functional capacity have been further characterized with the SLAM surface marker CD150, with both CD150− and CD150+ SP subpopulations contributing to distinct lineages that demonstrate distinct proliferative states (115).

Attempts to enrich for SP cells using other surface markers have resulted in the observations that CD9 did so in the porcine system (116) and Tie2+ cells obtained from murine bone marrow also highly enriched for SP+ hematopoietic stem cells. Tie2 is a receptor tyrosine kinase also expressed on endothelial cells. In adult murine bone marrow, Tie-2+ cells were shown to adhere to ligand (angiopoietin-1) expressing osteoblasts at the surface of trabecular bone (117), supporting the concept of the hematopoietic stem cell niche at that location (118,119). Other studies have shown that murine SP cells could be enriched about 5-fold by use of the surface marker CD105+ (endoglin), which was identified by a novel oligonucleotide microarray analysis only requiring 1 ng of RNA. More recently, it was reported that the reconstitutive activity of murine SP cells could be enriched in cells expressing the endothelial protein C receptor CD201 on the cell surface (120). This marker was discovered by comparison of the differential gene expression profile of purified versus non-SP cells using Affymetrix microarrays.

SP cells have been obtained from numerous solid tissue sources and species (113,121). For example, SP cells identified in the murine lung appear to have both mesenchymal and epithelial potential (122). In other studies, SP cells obtained from murine muscle were shown to express Sca-1, but lacked the CD117+, CD43+ and CD45+ immunophenotype seen in bone marrow. Similarly, Sca-1+, cKit-CD45− CD31− SP cells have been isolated

from murine myometrium with the potential for adipogenesis and/or smooth muscle (123). SP cells have been determined to be responsible for normal ovarian regeneration, and found in label retaining cells in a murine model (124). Muscle derived SP cells were capable of reconstituting the hematopoietic compartment, but not as efficiently as BM derived SP cells, suggesting the importance of micro-environmental factors on plasticity-related SP cell function (125). SP cells have also been isolated from adult rat kidney (126), murine liver (127) testis (128), skin (129) and mammary gland (130). SP cells have been isolated from adult human peripheral blood and characterized expressing relatively high levels of CD45, CD59, CD43+, CD49d, CD31and lacking CD34. Functional studies in immunodeficient mice and *in-vitro* assays suggested that these cells were further differentiated relative to multipotent murine marrow SP cells, only giving rise to lymphoid cells (25). It is possible that hematopoietic multipotential capacity might reside within ALDH+ CD34- cells rather than the SP CD34- cell compartment, in humans (131).

At this time, it is appears that isolation of SPcells from these various tissues seems to enrich for residenttissue stem or progenitor cells, but not necessarily exclusively so. Recent advances in two-photon microscopy and software permit the study of SP cells in tissue culture, opening up their microenvironmental interactions in heterogeneous cultures without disruption (132). With further such in-situ study, increased clarification of the role of SP cells in development will hopefully become further evident.

Rhodamine 123—Rhodamine 123 is a non-toxic lipophilic cationic fluorescent dye which binds within the mitochondria of living cells, and similar to Hoechst is effluxed efficiently by a p-glycoprotein/ATP transporter. It has been used in experiments with Hoechst 33342 to identify and separate long term repopulating cells from murine bone marrow (133).

Cell Tracking, Proliferation, Signaling & Reporter Genes

The lipophilic membrane binding PKH and protein-binding CSFE (carboxyfluorescein diacetate, succinimidyl ester) dyes (Table 1) have been found to be useful for *in vitro* cell labeling, in vitro proliferation studies and long term, in vivo cell tracking. Upon entering cells, these dyes diffuse throughout the cell membrane (PKH) or cytoplasm (CSFE). As the cells divide, the fluorescent emissions are split equally between the daughter cells resulting in diminished signal detection by flow cytometry. This division, and resultant signal reduction occurs with each subsequent cell division. The ability to track cell division in conjunction with cell surface markers affords stem cell researchers with an essential tool to study experimental populations over time

Green fluorescent protein (GFP) is a 238 amino acid protein obtained initially from the bioluminescent jellyfish *Aequorea victoria*, whose gene can be introduced by viral vector or local injection into organisms (134). This has been very useful as a reporter gene, and many mammalian and non-mammalian cells have been created using GFP as a marker, although caution is warranted regarding strain specificity, resistance to fixation and it's lack of ubiquitous penetration into all tissue (135). Homologous proteins with disparate spectral characteristics including cyan (CFP) yellow-green (YFP) orange (DsRed and DsRed Express) and orange-red (HcRed) were subsequently developed (Table 1), increasing the available spectral breath of reporter genes for molecular studies that interface with flow cytometry (16). It is likely that phospho-specific protein phosphorylation and cellular signaling studies will be incorporated into the study of stem cells as these techniques mature (136).

Cancer stem cells and Flow Cytometry—The hypothesis of cancer stem cells is based upon the observation that not all cells derived from a tumor have the capacity to maintain

malignant growth. Rather, there appears to be a more exclusive pool of stem cells that are targeted by malignant transformation that are responsible for the ultimate success of the tumor. Similar to normal stem cells, cancer stem cells have the potential to self-renew, forming additional tumor cells of similar phenotype, while also giving rise to other tumor cells with more limited proliferative potential. This was initially demonstrated in the context of human acute myeloid leukemia by transplanting purified $CD34^{bright}$+CD38− cells derived from FAB characterized tumors and recovering the tumor from a NOD/SCID model (137). Subsequent studies suggested that the putative normal human hematopoietic stem cell expressing CD34+CD38−CD90+CD117+CD123− could be distinguished from it's malignant leukemic counterpart, which was CD34+CD38−CD90−CD117−CD123+ (138), although the characterization of CD90 expression is controversial (139).

The principle of a potential leukemic stem cell was extended to findings in epithelial breast tumors, where $CD44+CD24^{-/low}$ Lin^{neg} cells were found to be the tumor initiating cells (140) and in neural tumors where CD133+ nestin+ cells were identified as brain tumor stem cells (141). Similar to normal neural stem cells, brain cancer stem cells were determined to reside in perivascular niches that maintained the stem-like properties of these cancer cells, supporting an important interaction between the cell of origin and it's microenvironment (142). All these studies demonstrated the crucial importance of combining carefulcell sorting with functional assays since the distinction between the tumor initiating cells was based on specifically identified immunophenotypic differences between cell types.

Distinct from using cell surface markers, 'functionally identified' human SP cancer cells have been found in the central nervous system (143,144) as well as from numerous other tumors such as those from the hematopoietic system (145), prostate (146), ovary (147) and gastrointestinal tract (148).

By way of caution in interpreting these and other studies based upon xenotransplantation models, the numerous solid organ tumors described by combinations of CD44, CD24 CD133 and epithelial surface antigen (ESA) is extensive, and rather than specifying a particular *bona fide* cancer stem cell, might rather enrich for cells with the functional capacity to engraft into the immunodeficient murine model milieu often used by researchers (149,150,151).

Conclusion

The use of flow cytometry in stem cell research requires high levels of stringency and as 'fool-proof' techniques as possible, since often the numbers of cell populations of interest are relatively small, compared to those in other fields of study. Due to these small numbers of cells, it is advantageous to take advantage of the benefits of contemporary instruments and multiple reagent combinations to learn the maximum possible about these populations. The new software tools described in this review should further aid these endeavors.

While the convergence of improved hardware, reagents and software permit this capacity, the techniques to reproducibly stain cells with numerous directly conjugated fluorochromes is not yet at a "turn-key" stage. Simply consulting a table of dye excitation and emission maxima and matching these to band-pass filter specifications and excitation sources are the first step, but itself insufficient to achieve reliable polychromatic capacity. Initial problems, such as potential dye-dye interactions on the surface of cells, the stability of tandem conjugates, changes in background staining and potential cell-surface antigen steric problems need to be fully understood. While the need for calibration controls and compensation matrices presently require far more care than routine 4-color work, most of these obstacles have been sufficiently surmounted.

A variety of issues must be considered to bring reliable polychromatic flow cytometry into routine use in the stem cell laboratory. For example, certain cyanine dyes non-specifically stick to B-cells and macrophages and thus must be carefully utilized if these cells are present. The newly available Alexa dyes may serve as suitable substitutes for the cyanine dyes. It is important to remember that manufactured lots of tandem-conjugated antibodies may have disparate compensation needs due to variable ratios of donor and acceptor molecules and need be carefully monitored; improved quality control from the manufacturers of these reagents will be welcome. In addition to cell surface staining, stem cell analysis might require inquiry into intra-nuclear (e.g., TdT), cytoplasmic (e.g. cytokine, activation pathway, MPO) antigens and cell signaling proteins. For these it is important to work with good negative and positive controls. Identification and discrimination of viable cells has recently been improved by use of the cellular amine-binding LIVE/DEAD reactive dyes (Table 1;152). These dyes are available with a variety of excitation and associated emission capacities, permitting their use with numerous instrument platforms when analyzing paraformaldehyde fixed cells. The nucleic-acid binding propidium iodide, ethidium monoazide, 7-aminoactinomycin-D, DAPI or cytoplasmic membrane specific phosphatidylserine ligands (annexin V) remain useful viability reagents for live cell sorting.

From a practical perspective, there are numerous worthwhile advantages to perfecting a polychromatic staining protocol, over more typical 4-color staining protocols. These include obtaining improved data from hypo-cellular specimens, increased information about antigenic co-expression and the built-in quality control of multiple markers present in the same staining tube. From a reagent cost-containment perspective, the need to duplicate the use of monoclonal antibodies in large four-color panels is obviated when unconstrained to a 4-color limitation; this also results in overall decrease in the use of ancillary staining [e.g. lyse, fixation] reagents. The need to use fewer staining tubes per sample will result in an overall increase in cytometer throughput, although post-acquisition analysis is increased. Routine ‘CD45 gating’ to exclude erythrocytes and debris from viable leukocytes also becomes a more realistic and cost effective option when there are numerous immunofluorescent parameters to work with. Finally, cell function, specificity and state of activation may be more easily understood by simultaneously incorporating flow-based cell-cycle, proliferation, cytokine and tetramer expression studies into polychromatic staining protocols.

It is important to appreciate that the goal of polychromatic cytometry and described new advanced instruments analytical tools is to *simplify and enhance* the understanding of stem cells. The information content available increases geometrically with each additional parameter and uncovers co-expressions otherwise unavailable to the cell biologist. The cytometric community needs to take the lead in the exploration and introduction of the new hardware, reagent and software tools newly available to us. It is felt the advantages of polychromatic cytometry far outweigh some present problems, which are surmountable. It is also worthwhile to note that new technologies such as the Amnis Image Stream expand the breath of information available to traditional flow cytometry. Simply put, it is good research practice to obtain the increased depth of information possibly by implementing these new technologies. We feel that the quality of data presented here demonstrates their practical feasibility, proof-of-principle and future possibilities.

Acknowledgments

Drs. C.B. Bagwell, T. Dubrovsky, R. Hulspas, and R. Sutherland are acknowledged for their various contributions and/or discussions regarding this manuscript.

References

1. Till JE, McCulloch EA. A direct measurement of the radiation sensitivity of normal mouse bone marrow cells. Radiat Res. 1961; 14:1419–1430.
2. Metcalf, D.; Moore, MAS. Haemopoietic Cells. North Holland: Amsterdam; 1971. p. 123-146.
3. Schofield R. The relationship between the spleen colony-forming cell and the haematopoietic stem cell. A hypothesis Blood Cells. 1978; 4:7–25.
4. Kawai T, Cosimi AB, Spitzer TR, Tolkoff-Rubin N, Suthanthiran M, Saidman SL, Shaffer J, Preffer FI, Ding R, Sharma V, Fishman JA, Dey B, Ko D, Hertl M, Goes NB, Wong W, Williams WW, Colvin RB, Sykes M, Sachs DH. Tolerance to HLA-Mismatched Renal Allografts Following Combined Kidney and Bone Marrow Transplantation. N Engl J Med. 2008; 358:353–361. [PubMed: 18216355]
5. Weissman IL. Translating stem and progenitor cell biology to the clinic: barriers and opportunities. Science. 2000; 287:1442–1446. [PubMed: 10688785]
6. Sweet, RO. Stanford Univ Tech Report 1722–1 Report SU-SEL-64–004. Defense Document Center; Washington. D.C: 1964.
7. Fulwyler MJ. Electronic separation of biological cells by volume. Science. 1965; 150:910–911. [PubMed: 5891056]
8. Kamentsky LA, Melamed MR, Derman H. Spectrophotometer: New instrument for ultrarapid cell analysis. Science. 1965; 150:630–631. [PubMed: 5837105]
9. Van Dilla MA, Trujillo TT, Mullaney PF, Coulter JR. Cell microfluorimetry: A method for rapid fluorescence measurement. Science. 1969; 163:1213–1214. [PubMed: 5812751]
10. Hulett HR, Bonner WA, Barrett J, Herzenberg LA. Cell sorting: automated separation of mammalian cells as a function of intracellular fluorescence. Science. 1969; 166:747–749. [PubMed: 4898615]
11. Van Dilla, MA.; Dean, PN.; Laerum, OD.; Melamed, ML. Flow Cytometry: Instrumentation and Data Analysis. New York: Academic Press; 1985.
12. Preffer, FI.; Colvin, RB. Analysis and Sorting by Flow Cytometry: Applications to the Study of Human Disease. In: Pretlow, TG., II; Pretlow, TP., editors. Cell Separation –Methods and Selected Applications. New York: Academic Press; 1987. p. 311-347.
13. Preffer, FI. Flow Cytometry. In: Colvin, RB.; Bhan, AK.; McCluskey, RT., editors. Diagnostic Immunopathology. New York: Raven Press; 1995. p. 725-749.
14. Melamed, MR.; Lindmo, T.; Mendelsohn, ML. Flow Cytometry and Sorting. New Jersey: John Wiley and Sons; 1990.
15. Baumgarth N, Roederer M. A practical approach to multicolor flow cytometry for immunophenotyping. J Immunol Methods. 2002; 243:77–97. [PubMed: 10986408]
16. Shapiro, HM. Practical Flow Cytometry. New Jersey: John Wiley and Sons; 2003.
17. Mahnke YD, Roederer MR. Optimizing a multicolor immunophenotyping assay. Clin Lab Med. 2007; 27:469–485. [PubMed: 17658403]
18. De Rosa SC, Roederer M. Eleven-color flow cytometry. A powerful tool for elucidation of the complex immune system. Clin Lab Med. 2001; 21:697–712. [PubMed: 11770282]
19. Perez OD, Nolan GP. Simultaneous measurement of multiple active kinase states using polychromatic flow cytometry. Nat Biotechnol. 2002; 20:155–162. [PubMed: 11821861]
20. De Rosa SC, Brenchley JM, Roederer M. Beyond six colors: a new era in flow cytometry. Nature Med. 2003; 9:112–117. [PubMed: 12514723]
21. Wood B. 9-color and 10-color flow cytometry in the clinical laboratory. Arch Pathol Lab Med. 2006; 130:680–690. [PubMed: 16683886]
22. Cabana R, Frolova EG, Kapoor V, Thomas RA, Krishan A, Telford WG. The minimal instrumentation requirements for hoechst side population analysis: Stem cell analysis on low-cost flow cytometry platforms. Stem Cells. 2006; 24:2573–2581. [PubMed: 16888279]
23. Kapoor V, Subach FV, Koslov VG, Grudinin A, Verkhusha VV, Telford WG. New lasers for flow cytometry: filling the gaps. Nature Methods. 2007; 4:678–679. [PubMed: 17762872]

24. Goodell MA, Brose K, Paradis G, Conner AS, Mulligan RC. Isolation and functional properties of murine hematopoietic stem cells that are replicating in vivo. J Exp Med. 1996; 183:1797–1806. [PubMed: 8666936]
25. Preffer FI, Dombkowski D, Sykes M, Scadden D, Yang Y. Lineage negative side population [SP] cells with restricted hematopoietic capacity circulate in normal human adult blood. Immunophenotypic and functional characterization. Stem Cells. 2002; 20:417–427. [PubMed: 12351812]
26. Stewart CC, Woodring ML, Podniesinski E, Grey B. Flow Cytometer in the Infrared: Inexpensive Modifications to a Commercial Instrument. Cytometry A. 2005; 67A(104):104–111. [PubMed: 16163692]
27. Parks DR, Roederer M, Moore WA. A new "logical" display method avoids deceptive effects of logarithmic scaling for low signals and compensated data. Cytometry A. 2006; 69A:541–551. [PubMed: 16604519]
28. Herzenberg LA, Tung J, Moore WA, Herzenberg LA, Parks DR. Interpreting flow cytometry data: a guide for the perplexed. Nature. 2006; 7:681–685.
29. Wood JCS, Hoffman RA. Evaluating fluorescence sensitivity on flow cytometers: An overview. Cytometry. 1998; 33:256–259. [PubMed: 9773888]
30. Wood JCS. Fundamental flow cytometer properties governing sensitivity and resolution. Cytometry. 1998; 33:256–259. [PubMed: 9773888]
31. Preffer, FI.; Dombkowski, D.; Dubrovsky, T.; Dorn, M.; Quaglioroli, R.; Leahy, K.; Duckett, L.; Ziganti, S. The Use of Polychromatic Flow Cytometry in Diagnostic Hematopathology. CCS Long Beach; CA: 2006. Abstract #1452
32. Duckett, L.; Dombkowski, D.; Ziganti, S.; Matsuyama, D.; Preffer, F. ISAC. Vol. XXIII. Quebec City; Canada: 2006. Introduction of 7-Laser LSRII and 5-Laser FACSAria. Abstract #261
33. Preffer, FI.; Dombkowski, D.; Cannizzo, E.; Nasraty, Q.; Dubruvsky, T.; Duckett, L.; Farrigno, P.; Ziganti, S. ISAC. Vol. XXIV. Budapest; Hungary: 2006. Thermo-immunology: infra-red Excitation of monoclonal antibody conjugates and advantage of excitation with special 7-laser LSR. Abstract# 554
34. Hyun W, Daniel RH, Hotz CZ, Bruchez M. Nanocrystals as multicolor single excitation probes for flow and image cytometry. Cytometry Supp. 2000; 10:182.
35. Akerman ME, Chan W, Laakkonen P, Bhatia SN, Ruoslahti E. Nanocrystal targeting in vivo. Proc Natl Sci Acad USA. 2002; 99:12617–12621.
36. Nisman R, Dellaire G, Ren Y, Li R, Bazett-Jones. Application of quantum dots as probes for correlative fluorescence conventional and energy-filtered transmission electron microscopy. J Histochem Cytochem. 2004; 52:12–18.
37. Nyk M, Kumar R, Ohulchanskyy TY, Bergey EJ, Prasad PN. High contrast in vitro and in vivo photoluminescence bioimaging using near infrared to near infrared up-conversion in Tm3+ and Yb3+ doped fluoride nanophosphors. Nanoletters. 2008; 8:3834–3838.
38. Boedigheimer MJ, Ferbas J. Mixture modeling approach to flow cytometry data. Cytometry A. 2008; 73A:421–429. [PubMed: 18383311]
39. Rogers WT, Moser AR, Holyst HA, Bantly A, Mohler ER III, Scangas G, Moore JS. Cytometric fingerprinting: quantitative characterization of multivariate distributions. Cytometry A. 2008; 73A: 430–441. [PubMed: 18383310]
40. Finn WG, Carter KM, Raich R, Stoolman LM, Hero AO. Analysis of clinical flow cytometric immunophenotyping data by clistering on statistical manifolds: treating flow cytometry data as high-dimensional objects. Cytometry B. 2009; 76B:1–7.
41. Roederer M, Moore W, Treister AS, Hardy RR, Herzenberg LA. Probability binning comparison: a metric for quantitating multivariate distribution differences. Cytometry. 2001; 45:47–55. [PubMed: 11598946]
42. Petrausch U, Haley D, Miller W, Floyd K, Urba WJ, Walker E. Polychromatic flow cytometry: A rapid method for the reduction and analysis of complex multiparameter data. Cytometry A. 2006; 69A:1162–1173. [PubMed: 17089357]
43. Murphy RF. Automated identification of subpopulations in flow cytometric list mode data using cluster analysis. Cytometry. 1985; 6:302–309. [PubMed: 4017796]

44. Wegman EJ, Luo Q. High dimensional clustering using parallel coordinates and the grand tour. Comput Sci Stat. 1997; 28:352–360.
45. Streit M, Ecker RC, Osterreicher K, Steiner GE, Bischof H, Bangert C, Kopp T, Rogojanu R. 3D parallel coordinate systems--a new data visualization method in the context of microscopy-based multicolor tissue cytometry. Cytometry A. 2006; 69A:601–611. [PubMed: 16680710]
46. Johansson J, Ljung P, Jern M, Cooper M. Revealing structure in visualizations of dense 2D and 3D parallel coordinates. Information Visualization. 2006; 5:125–136.
47. Breaking the Dimensionality Barrier. Laboratory Hematology Practice. 2008; Chapter 12
48. Vacca, G.; Yee, MW.; Goldblatt, NR.; Lui, WW.; Junnarkar, MR.; Kendall, RG.; Hulett, FM. ISAC. Vol. XXIV. Budapest; 2008. Laser rastering:a new high-speed approach to flow cytometry. Abstract #5
49. Goddard G, Martin JC, Graves SW, Kaduchak G. Ultrasonic particle-concentration for sheathless focusing of particles for analysis in a flow cytometer. Cytometry A. 2006; 69A:66–74. [PubMed: 16419065]
50. Leary JF. Ultra high-speed Sorting. Cytometry A. 2005; 67A:76–85. [PubMed: 16163688]
51. http://www.cytonome.com/ci/183/Overview_of_Gigasort_Technology/
52. Gregori, G.; Valery, P.; Bartek, R.; Robinson, PJ. ISAC. Vol. XXIV. Budapest; Hungary: 2006. Hyperspectral flow cytometry. Abstract# 554
53. Toner M, Irimia D. Blood-on-a-chip. Ann Rev Biomed Eng. 2005; 7:77–103. [PubMed: 16004567]
54. Furuki, M.; Imanishi, S.; Shinoda, M.; Tsuboi, N.; Morita, Y.; Yamazaki, Y.; Nakauchi, H. ISAC. Vol. XXIV. Budapest; Hungary: 2006. Laser scanning spectral flow cytometry with microfluidic chip. Abstract# 554
55. Koller MR, Hanania EG, Stevens J, Eisfeld TM, Sasaki GC, Fieck A, Palsson BO. High-throughput laser-mediated in situ cell purification with high purity and yield. Cytometry A. 2004; 61A:153–161. [PubMed: 15382147]
56. Woll PS, Morris JK, Painschab MS, Marcus RK, Kohn AD, Biechele TL, Moon RT, Kaufman DS. Wnt signaling promotes hematoendothelial cell development from human embryonic stem cells. Blood. 2007; 111:122–131. [PubMed: 17875805]
57. Guzman ML, Li X, Corbett CA, Rossi RM, Bushnell T, Liesveld JL, Hebert J, Yopung F, Jordan CT. Rapid and selective death of leukemia stem and progenitor cells induced by the compound 4-benzyl 2-methyl 1 2 4-thiadiazolidine 3 5 dione (TDZD-8). Blood. 2007; 110:4436–4444. [PubMed: 17785584]
58. Ratajczak MZ, Zuba-Surma EK, Wysoczynski M, Wan W, Ratajczak J, Wojakowski W, Kucia M. Hunt for pluripotent stem cell- Regenerative medicine search for almighty cell. J Autoimmunity. 2008; 30:151–162. [PubMed: 18243661]
59. Zuba-Surma EK, Kucia M, Ratajczak J, Ratajczak. “Small stem cells” in adult tissues: very small embryonic-like stem cells stand up! Cytometry A. 2009; 75A:4–13. [PubMed: 18988270]
60. Challen GA, Boles N, Lin KK-Y, Goodell MA. Mouse hematopoietic stem cell identification and analysis. Cytometry A. 2009; 79A:14–24. [PubMed: 19023891]
61. Spangrude GJ, Muller-Sieburg CE, Heimfeld S, Weissman IL. Two rare populations of mouse Thy-1lo bone marrow cells repopulate the thymus. J Exp Med. 1986; 167:1671–1683. [PubMed: 2896758]
62. Muller-Sieburg CE, Whitlock CA, Weissman IL. Isolation of two early B lymphocyte progenitors from mouse marrow: A committed pre-pre-B cell and a clonogenic Thy-1-low hematopoietic stem cell. Cell. 1986; 44:653–662. [PubMed: 2868799]
63. Sutherland HJ, Eaves CJ, Eaves AC, Dragowska W, Lansdorp PM. Characterization and partial purification of human marrow cells capable of initiating long-term hematopoiesis in vitro. Blood. 1989; 74:1563–1570. [PubMed: 2790186]
64. Adolfsson J, Borge OJ, Bryder D, Theilgaard-Monch K, Astrand-Grundstrom I, Sitnicka E, Sasaki Y, Jacobsen SE. Upregulation of Flt3 expression within the bone marrow Lin( )Sca1(+)c-kit(+) stem cell compartment is accompanied by loss of self-renewal capacity. Immunity. 2001; 15:659–669. [PubMed: 11672547]
65. Yang L, Bryder D, Adolfsson J, Nygren J, Mansson R, Sigvardsson M, Jacobsen SE. Identification of Lin( )Sca1(+)kit(+)CD34(+)Flt3-short-term hematopoietic stem cells capable of rapidly

reconstituting and rescuing myeloablated transplant recipients. Blood. 2005; 105:2717–2723. [PubMed: 15572596]

66. Kiel MJ, Yilmaz OH, Iwashita T, Yilmaz OH, Terhorst C, Morrison SJ. SLAM family receptors distinguish hematopoietic stem and progenitor cells and reveal endothelial niches for stem cells. Cell. 2005; 121:1109–1121. [PubMed: 15989959]
67. Sutherland DR, Marsh JC, Davidson J, Baker MA, Keating A, Mellors A. Differential sensitivity of CD34 epitopes to cleavage by *Pasturella haemolytica* glycoprotease: implications for purification of CD34-positive progenitor cells. Exp. Hematol. 1992; 20:590–599.
68. Sutherland DR, Keeney M. Re: Selection of stem Cells by using antibodies that target different CD34 epitopes yields different pattern of T-cell differentiation. Stem Cells. 2007; 25:2385–2386. [PubMed: 17569789]
69. De Wynter EA, Buck D, Haywood HR, Coutinho LH, Clayton A, Rafferty JA, Burt D, Guenechea G, Nueren JA, Gagen D, Fairbaim LJ, Lord BI, Testa NG. CD34+AC13+ cells isolated from cord blood are highly enriched in long-term culture-initiating cells and dendritic cell progenitors. Stem Cells. 1998; 16:387–396. [PubMed: 9831864]
70. Murray LJ, Bruno E, Uchida N, Hoffman R, Nayar R, Yeo EL, Schuh AC, Sutherland DR. CD109 is expressed on a subpopulation of CD34+ cells enriched in hematopoietic stem and progenitor cells. Exp Hematol. 1999; 27:1282–1294. [PubMed: 10428505]
71. Majeti R, Park CY, Weissman IL. Identification of a hierarchy of multipotent hematopoietic progenitors in human cord blood. Cell Stem Cell. 2007; 1:635–645. [PubMed: 18371405]
72. Krause DS, Ito T, Fackler MJ, Smith OM, Collector MI, Sharkis SJ, May WS. Characterization of murine CD34 a marker for hematopoietic progenitor and stem cells. Blood. 1994; 84:691–701. [PubMed: 7519070]
73. Cheng J, Baumhueter S, Cacalano G, Carver-Moore K, Thibodeaux H, Broxmeyer HE, Cooper S, Hague N, Moore M, Lasky LA. Hematopoietic defects in mice lacking the sialomucin CD34. Blood. 1996; 87:479–490. [PubMed: 8555469]
74. Kiel MJ, Yilmaz OH, Iwashita T, Morrison SJ. SLAM family receptors distinguish hematopoietic stem and progenitor cells and reveal endothelial niches for stem cells. Cell. 2005; 121:1109–1121. [PubMed: 15989959]
75. Yilmaz OH, Kiel MJ, Morrison SJ. SLAM family markers are conserved among hematopoietic stem cells from old and reconstituted mice and markedly increase their purity. Blood. 2006; 107:924–930. [PubMed: 16219798]
76. Shmelkov SV, St Clair R, Lyden D, Raffi S. AC133/CD133/Prominin-1. Int J Biochem Cell Bio. 2004; 37:715–719. [PubMed: 15694831]
77. Hess DA, Wirthlin L, Craft TP, Herrbrich PE, Hohm SA, Lahey R, Eades WC, Creer MH, Nolta JA. Selection based on CD133 and high aldehyde dehydrogenase activity isolates long-term reconstituting human hematopoietic stem cells. Blood. 2006; 107:2162–2169. [PubMed: 16269619]
78. Kusumbe AP, Mali AM, Bapat SA. CD133 expressing stem cells associated with ovarian metastases establish an endothelial hierarchy and contribute to tumor vasculature. Stem Cells Express. 2009 doi: 10.1634.
79. Miraglia S, Godfrey W, Yin AH, Atkins K, Warnke R, Holden JT, Bray RA, Waller EK, Buck DW. A novel five-transmembrane hematopoietic stem cell antigen: isolation characterization and molecular cloning. Blood. 1997; 90:5013–5021. [PubMed: 9389721]
80. Matsumoto K, Yasui K, Yamashita N, Horie Y, Yamada T, Tani Y, Shibata H, Nakano T. In Vitro proliferation potential of AC133 positive cells in peripheral blood. Stem Cells. 2000; 18:196–203. [PubMed: 10840073]
81. Summers YJ, Heyworth CM, De Wynter EA, Hart CA, Chang J, Testa NG. AC133+G_0 cells from cord blood show a high incidence of long-term culture-initiating cells and a capacity for more than 100 million-fold amplification of colony-forming cells in vitro. Stem Cells. 2004; 22:704–715. [PubMed: 15342935]
82. Kanayasu-Toyoda T, Yamaguchi T, Oshizawa T, Hayakawa T. CD31 (PECAM-1) bright cells derived from AC133-positive cells in human peripheral blood as endothelial-precursor cells. J Cell Physiol. 2003; 195:119–129. [PubMed: 12599215]

83. Belicchi M, Pisati F, Lopa R, Porretti L, Fortunato F, Sironi M, Scalamogna M, Parati EA, Bresolin N, Torrente Y. Human skin-derived stem cells migrate throughout forebrain and differentiate into astrocytes after injection into adult mouse brain. J Neurosci Res. 2004; 77:475–486. [PubMed: 15264217]
84. Buhring H-J, Kuci S, Conze T, Rathke G, Bartolovic K, Grunebach F, Scherl-Mostageer M, Brummendorf TH, Schweifer N, Lammers R. CDCP1 identifies a broad spectrum of normal and malignant stem/progenitor cell subsets of hematopoietic and nonhematopoietic origin. Stem Cells. 2004; 22:334–243. [PubMed: 15153610]
85. Yarden Y, Kuang WJ, Yang-Feng T, Coussens L, Munemitsu S, Dull TJ, Chen E, Schlessinger J, Francke U, Ullrich A. Human proto-oncogene c-kit: a new cell surface receptor tyrosine kinase for an unidentified ligand. EMBO J. 1987; 6:3341–3351. [PubMed: 2448137]
86. Vliagoftis H, Worobec AS, Metcalfe DD. The protooncogene c-kit and c-kit ligand in human disease. J Allergy Clin Immunol. 1997; 100:435–440. [PubMed: 9338533]
87. Huss R, Hong DS, Beckham C, Kimball L, Myerson DH, Storb R, Deeg HJ. Ultrastructural localization of stem cell factor in canine marrow-derived stromal cells. Exp Hematol. 1995; 23:33–40. [PubMed: 7527783]
88. Natali PG, Nicotra MR, Sures I, Santoro E, Bigotti A, Ullrich A. Expression of c-kit receptor in normal and transformed human nonlymphoid tissues. Cancer Res. 1992; 52:6139–6143. [PubMed: 1384954]
89. Edling CE, Hallberg B. C-Kit- a hematopoietic cell essential receptor tyrosine kinase. Int J Biochem Cell Biol. 2007; 39:1995–1998. [PubMed: 17350321]
90. Krause DS, Van Etten RA. Right on target:eradicating leukemic stem cells. Trends Mol Med. 2007; 13:470–481. [PubMed: 17981087]
91. Krause DS, Van Etten RA. Tyrosine kinases as targets for cancer therapy. N Engl J Med. 2005; 353:172–187. [PubMed: 16014887]
92. Haeryfar SMM, Hoskin DW. Thy-1: More than a mouse pan-T cell marker. J Immunol. 2004; 173:3581–3588. [PubMed: 15356100]
93. Masson NM, Currie IS, Terrace JD, Garden OJ, Parks RW, Ross JA. Hepatic progenitor cells in human fetal liver express the oval cell marker Thy-1. Am J Physiol Gastrointest Liver Physiol. 2006; 291:G45–G54. [PubMed: 16769813]
94. Chen CZ, Li M, de Graaf D, Monti S, Gottgens B, Sanchez MJ, Lander ES, Golub TR, Green AR, Lodish HF. Identification of endoglin as a functional marker that defines long-term repopulating hematopoietic stem cells. Proc Natl Acad Sci USA. 2002; 99:15468–15473. [PubMed: 12438646]
95. Fonsatti E, Maio M. Highlights on endoglin (CD105): from basic findings towards clinical applications in human cancer. J Translational Med. 2004; 2:8–25.
96. Le Blanc K, Ringden O. Immunobiology of human mesenchymal stem cells and future use in hematopoietic stem cell transplantation. Biol Blood Marrow Tr. 2005; 11:321–334.
97. Aggarwal S, Pittenger MF. Human mesenchymal stem cells modulate allogeneic immune cell responses. Blood. 2005; 105:1815–1822. [PubMed: 15494428]
98. Weisel KC, Yildirim S, Schweikle E, Kanz L, Mohle R. Effect of FLT3 inhibition on normal hematopoietic progenitor cells. Ann NY Acad Sci USA. 2007; 1106:190–196.
99. Christensen JL, Weissman IL. Flk-2 is a marker in hematopoietic stem cell differentiation: a simple method to isolate long-term stem cells. Proc Natl Acad Sci USA. 2001; 98:14541–14546. [PubMed: 11724967]
100. Gordon MY, Goldman JM, Gordon-Smith EC. 4-hydroperoxycyclophosphamide inhibits proliferation by human granulocyte-macrophage colony-forming cells (GM-CFC) but spares more primitive progenitor cells. Leuk Res. 1985; 9:1017–1019. [PubMed: 4046632]
101. Jones RJ, Barber JP, Vala MS, Collector MI, Kaufmann SH, Ludeman SM, Colvin OM, Hilton J. Assessment of aldehyde dehydrogenase in viable cells. Blood. 1995; 15:2742–2746. [PubMed: 7742535]
102. Hess DA, Meyerrose TE, Wirthlin L, Craft TP, Herrbrich PE, Creer MH, Nolta JA. Functional characterization of highly purified human hematopoietic repopulating cells isolated according to aldehyde dehydrogenase activity. Blood. 2004; 104:1648–1655. [PubMed: 15178579]

103. Storms RW, Green PD, Safford KM, Niedzwiecki D, Cogle CR, Colvin OM, Chao NJ, Rice HE, Smith CA. Distinct hematopoietic progenitor compartments are delineated by the expression of aldehyde dehydrogenase and CD34. Blood. 2005; 106:95–102. [PubMed: 15790790]
104. Corti S, Locatelli F, Papadimitriou D, Donadoni C, Salani S, Del Bo R, Strazzer S, Bresolin N, Comi GP. Identification of a primitive brain-derived neural stem cell population based on aldehyde dehydrogenase activity. Stem Cells. 2006; 24:975–985. [PubMed: 16293577]
105. Cai J, Cheng A, Luo Y, Mattson MP, Rao MS, Furukawa K. Membrane properties of rat embryonic multipotent neural stem cells. J Neurochemistry. 2004; 88:212–226.
106. Corti S, Locatelli F, Papadimitriou D, Donadoni C, Del Bo R, Strazzer S, Menozzi G, Salani S, Bresolin N, Comi GP. Transplanted ALDHhiSSClo neural stem cells generate motor neurons and delay disease progression of nmd mice an animal model of SMARD1. Hum Mol Genet. 2006; 15:167–187. [PubMed: 16339214]
107. Petersen TW, Ibrahim SF, Diercks AH, Van den Engh Ger. Chromatic shifts in the fluorescence emitted by murine thymocytes stained with hoechst 33342. Cytometry A. 2004; 60A:173–181. [PubMed: 15290718]
108. Arndt-Jovin DJ, Jovin TM. Analysis and sorting of living cells according to deoxyribonucleic acid content. J Histochem Cytochem. 1977; 25:585–589. [PubMed: 70450]
109. Zhou S, Schuetz JD, Bunting KD, Colapietro AM, Sampath J, Morris JJ, Lagutina I, Grosveld GC, Osawa M, Nakauchi H, Sorrentino BP. The ABC transporter Bcrp/ABCG2 is expressed in a wide variety of stem cells and is a molecular determinant of the side-population phenotype. Nature Med. 2001; 7:1028 – 1034. [PubMed: 11533706]
110. Bunting KD. ABC Transporters as phenotypic markers and functional regulators of stem cells. Stem Cells. 2002; 20:11–20. [PubMed: 11796918]
111. Ibrahim SF, Diercks AH, Petersen TW, van den Engh G. Kinetic analyses as a critical parameter in defining the side population (SP) phenotype. Experimental Cell Research. 2007; 313:1921–1926. [PubMed: 17428468]
112. Lin KK, Goodell MA. Purification of hematopoietic stem cells using the side population. Methods Enzymol. 2006; 420:255–264. [PubMed: 17161700]
113. Goodell MA, Rosenzweig M, Kim H, Marks DF, DeMaria MA, Paradis G, Grupp SA, Sieff CA, Mulligan RC, Johnson RP. Dye efflux studies suggest that hematopoietic stem cells expressing low or undetectable levels of CD34 antigen exist in multiple species. Nature Med. 1997; 12:1337–1345. [PubMed: 9396603]
114. Matsuzaki Y, Kinjo K, Mulligan RC, Okano H. Unexpectedly efficient homing capacity of purified murine hematopoietic stem cells. Immunity. 2004; 20:87–93. [PubMed: 14738767]
115. Weksberg DC, Chambers SM, Boles NC, Goodell MA. CD150- side population cells represent a functionally distinct population of long-term hematopoietic stem cells. Blood. 2008; 111:2444–2451. [PubMed: 18055867]
116. Heinz M, Huang C, Emery D, Giovino M, LeGuern A, Kurilla-Mahon B, Theodore P, Arn S, Sykes M, Mulligan R, Down J, Sachs DH, Goodell M. Use of CD9 expression to enrich for porcine hematopoietic progenitors. Exp Hematol. 2002; 30:809–815. [PubMed: 12135680]
117. Arai A, Hirao M, Ohmura H, Sato S, Matsuoka K, Takubo K, Ito K, Koh GY, Suda T. Tie2/angiopoietin-1 signaling regulates hematopoietic stem cell quiescence in the bone marrow niche. Cell. 2004; 118:149–161. [PubMed: 15260986]
118. Calvi LM, Adams GB, Weibrecht KW, Weber JM, Olson DP, Knight MC, Martin RP, Schipani E, Divieti P, Bringhurst FR, Milner LA, Kronenberg HM, Scadden DT. Osteoblastic cells regulate the haematopoietic stem cell niche. Nature. 2003; 425:841–846. [PubMed: 14574413]
119. Zhang J, Niu C, Ye L, Huang H, He X, Tong WG, Ross J, Haug J, Johnson T, Feng JQ, Harris S, Wiedemann LM, Mishina Y, Li L. Identification of the haematopoietic stem cell niche and control of the niche size. Nature. 2003; 425:836–841. [PubMed: 14574412]
120. Balazs AB, Fabian AJ, Esmon CT, Mulligan RC. Endothelial protein C receptor (CD201) explicitly identifies hematopoietic stem cells in murine bone marrow. Blood. 2006; 107:2317–2321. [PubMed: 16304059]
121. Challen GA, Little MH. A side order of stem cells: the SP phenotype. Stem Cells. 2006; 24:3–12. [PubMed: 16449630]

122. Majka SM, Beutz MA, Hagen M, Izzo AA, Voelkel N, Helm KM. Identification of novel resident pulmonary stem cells: Form and function of the lung side population. Stem Cells. 2005; 23:1073–1081. [PubMed: 15987674]
123. Szotek PP, Chang HL, Zhang L, Preffer F, Dombkowski D, Donahoe PK, Teixeira J. Adult mouse myometrial label-retaining cells divide in response to gonadotropin stimulation. Stem Cells. 2007; 25:1317–1325. [PubMed: 17289934]
124. Szotek P, Chang H, Brennand K, Fujino A, Pieretti-Vanmarcke R, Lo Celso C, Dombkowski D, Preffer F, Cohen K, Teixeira J, Donanhoe P. Normal Ovarian Surface Epithelial Label Retaining Cells Exhibit Stem/Progenitor Cell Characteristics. Proc Natl Acad Sci USA. 2008; 105:12469–12473. [PubMed: 18711140]
125. Gussoni E, Soneoka Y, Strickland CD, Buzney EA, Khan MK, Flint AF, Kunkel LM, Mulligan RC. Dystrophin expression in the mdx mouse restored by stem cell transplantation. Nature. 1999; 401:390–394. [PubMed: 10517639]
126. Iwatani H, Ito T, Imai E, Matsuzaki Y, Suzuki A, Yamato M, Okabe M, Hori M. Hematopoietic and nonhematopoietic potentials of Hoechst (low)/side population cells isolated from adult rat kidney. Kidney Int. 2004; 65:1604–1614. [PubMed: 15086898]
127. Wulf GG, Luo KL, Jackson KA, Brenner MK, Goodell MA. Cells of the hepatic side population contribute to liver regeneration and can be replenished by bone marrow stem cells. Haematologica. 2003; 88:368–378. [PubMed: 12681963]
128. Falciatori I, Borsellino G, Haliassos N, Boitani C, Corallini S, Battistini L, Bernardi G, Stefanini M, Vicini E. Identification and enrichment of spermatogonial stem cells displaying side-population phenotype in immature mouse testis. FASEB J. 2004; 18:376–388. [PubMed: 14688197]
129. Montanaro F, Liadaki K, Volinski J, Flint A, Kunkel LM. Skeletal muscle engraftment potential of adult mouse skin side population cells. Proc Natl Acad Sci USA. 2003; 100:9326–9341.
130. Welm BE, Tepera SB, Venezia T, Graubert TA, Rosen JM, Goodell MA. Sca-1(pos) cells in the mouse mammary gland represent an enriched progenitor cell population. Dev Biol. 2002; 245:42–56. [PubMed: 11969254]
131. Pearce DJ, Bonnet D. The combined use of Hoechst efflux ability and aldehyde dehydrogenase activity to identify murine and human hematopoietic stem cells. Exp Hematol. 2007; 35:1437–1446. [PubMed: 17656008]
132. Benchaouir R, Picot J, Greppo N, Rameau P, Stockholm D, Garcia L, Paldi A, Builhe CL. Combination of quantification and observation methods for study of “side population” cells in their “in vitro” microenvironment. Cytometry A. 2007; 71A:251–257. [PubMed: 17279573]
133. Wolf NS, Kone A, Priestley GV, Bartelmez SH. In vivo and in vitro characterization of long-term repopulating primitive hematopoietic cells isolated by sequential hoechst-33342-rhodamine-123 FACS selection. Exp Hematol. 1993; 21:614–622. [PubMed: 8513861]
134. Chalfie M, Tu Y, Euskirchen G, Ward WW, Prasher DC. Green fluorescent protein as a marker for gene expression. Science. 1994; 263:802–805. [PubMed: 8303295]
135. Swenson ES, Price JG, Brazelton T, Krause DS. Limitaitons of green fluorescent protein as a cell lineage marker. Stem Cells. 2007; 25:2593–2600. [PubMed: 17615263]
136. Krutzik PO, Irish JM, Nolan GP, Perez OD. Analysis of protein phosphorylation and cellular signaling events by flow cytometry: techniques and clinical applications. Clinical Immunol. 2004; 110:206–211. [PubMed: 15047199]
137. Bonnet D, Dick JE. Human acute myeloid leukemia is organized as a hierarchy that originates from a primitive hematopoietic cell. Nature Med. 1997; 3:730–737. [PubMed: 9212098]
138. Wang JC, Dick JE. Cancer stem cells: lessons from leukemia. Trends Cell Biol. 2005; 9:494–501. [PubMed: 16084092]
139. Brendel C, Mohr B, Schimmelpfennig C, Muller J, Bornhauser M, Schmidt M, Ritter M, Ehninger G, Neubauer A. Detection of cytogenetic aberrations both in CD90 (Thy-1)-positive and (Thy-1)-negative stem cell (CD34) subfractions of patients with acute and chronic myeloid leukemias. Leukemia. 1999; 13:1770–1775. [PubMed: 10557051]
140. Al-Hajj M, Wicha MS, Benito-Hernandez A, Morrison SJ, Clarke MF. Prospective identification of tumorigenic breast cancer cells. Proc Natl Sci Acad USA. 2003; 100:3983–3988.

141. Singh SK, Clarke ID, Terasaki M, Bonn VE, Hawkins C, Squire J, Dirks PB. Identification of a cancer stem cell in human brain tumors. Cancer Res. 2003; 63:5821–5828. [PubMed: 14522905]

142. Gilbertson RJ, Gutmann DH. Tumorigenesis in the Brain: Location location location. Cancer Res. 2007; 67:5579 – 5582. [PubMed: 17575119]

143. Kondo T, Setoguchi T, Taga T. Persistence of a small subpopulation of cancer stem-like cells in the C6 glioma cell line. Proc Nat Acad Sci USA. 2004; 101:781–786. [PubMed: 14711994]

144. Seigel GM, Campbell LM, Narayan M, Fernandez FG. Cancer stem cell characteristics in retinoblastoma. Mol Vis. 2005; 11:729–737. [PubMed: 16179903]

145. Wulf GG, Wang RY, Kuehnle I, Weidner D, Marini F, Brenner MK, Andreeff M, Goodell MA. A leukemic stem cell with intrinsic drug efflux capacity in acute myeloid leukemia. Blood. 2001; 98:1166–1173. [PubMed: 11493466]

146. Brown MD, Gilmore PE, Hart CA, Samuel JD, Ramani VAC, George NJ, Clark NW. Characterization of benign and malignant prostate epithelial hoechst 33342 side population. The Prostate. 2007; 67:1384–1386. [PubMed: 17639507]

147. Szotek PP, Pieretti-Vanmarcke R, Masiakos PT, Dinulescu DM, Connolly D, Foster R, Dombkowski D, Preffer F, Maclaughlin DT, Donahoe PK. Ovarian cancer side population defines cells with stem cell-like characteristics and Mullerian Inhibiting Substance responsiveness. Proc Natl Acad Sci USA. 2006; 103:11154–11159. [PubMed: 16849428]

148. Haraguchi N, Utsunomiya T, Inoue H, Mimori FTK, Bernard GF, Mori M. Characterization of a side population of cancer cells from human gastrointestinal system. Stem Cells. 2006; 24:506–513. [PubMed: 16239320]

149. Fillmore C, Kuperwasser C. Human breast cancer stem cell markers CD44 and CD24: enriching for cells with functional properties in mice or in man? Breast Cancer Research. 2007; 9:303–305. [PubMed: 17540049]

150. Kelly PN, Dakic A, Adams JM, Nutt SL, Strasser A. Tumor growth need not be driven by rare cancer stem cells. Science. 2007; 317:337. [PubMed: 17641192]

151. Die hard: are cancer stem cells the Bruce Willises of tumor biology? . Cytometry A. 2009; 79A: 67–74.

152. Perfetto SP, Chattopadhyay PK, Lamoreaux L, Nguyen R, Ambrozak D, Koup RA, Roederer M. Amine reactive dyes: an effective tool to discriminate live and dead cells in polychromatic flow cytometry. J Immunol Methods. 2006; 313:199–208. [PubMed: 16756987]

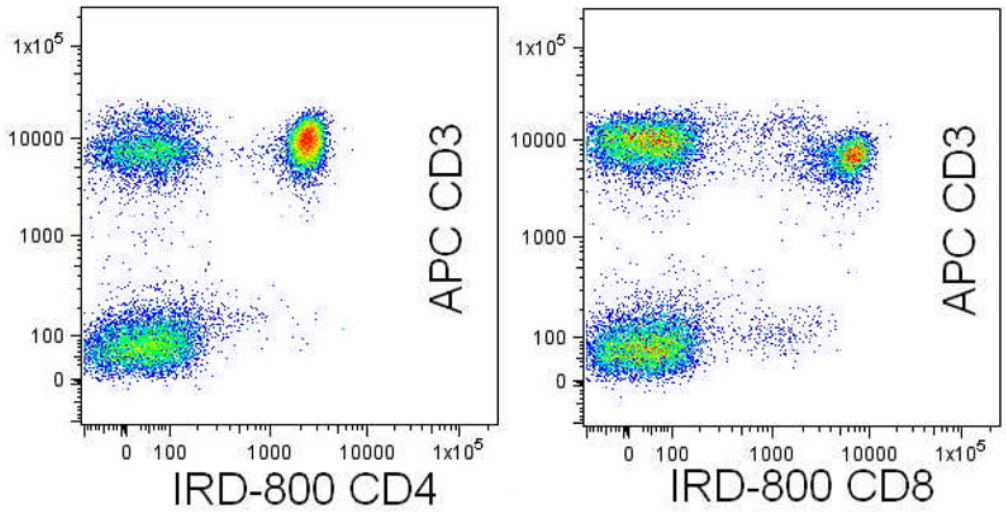

Figure 1. Thermo-Immunology

Demonstration of infra-red excitation of CD4 (left) and CD8 (right) monoclonal antibodies directly conjugated with LI-COR IR800 and captured by an infra-red selected Hamamatsu R3896MOD PMT. Peripheral blood was additionally stained with CD3-APC and CD45-FITC. This novel excitation line increases the repertoire of monoclonal antibody conjugate pairing available to the cytometrists and can also be used with infra-red excitable tracking dyes.

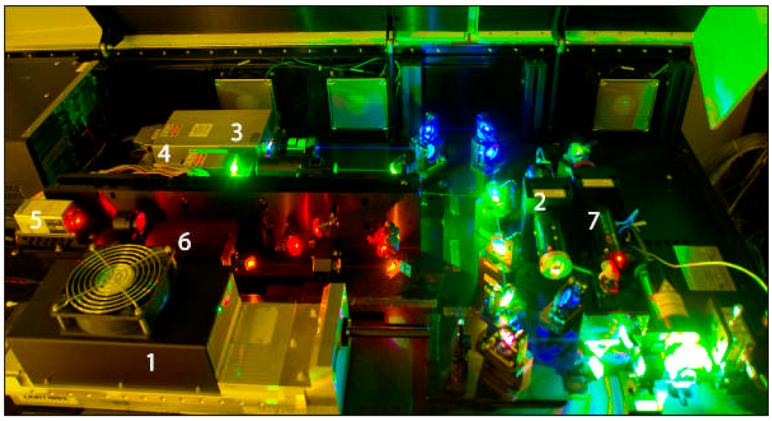

Figure 2. 7-Laser optical bench configuration

This experimental design platform permits multiple air-cooled lasers to be placed within a modestly sized laboratory benchtop configuration. Each of the lasers has independent steering optics that permits each beam to be accurately focused into the instrument's flow cell [lower right]. The power and wavelength of each laser, and the number of PMTs utilized is shown on the accompanying table.

	Laser	Wavelength [nm]	Style	Power [mw]	PMT Array	PMT#
1	UV	355	Mode Lock	20	Trigon	2
2	Violet	405	Diode Pumped Solid State	50	Octagon	8
3	Blue	488	Diode Pumped Solid State	20–100	Octagon	4
4	Green	532	Diode Pumped Solid State	40–150	Octagon	5
5	Yellow	594	Diode Pumped Solid State	50	Trigon	2
6	Red	638	Diode Pumped Solid State	40	Trigon	3
7	IR	785	Diode Pumped Solid State	25	Trigon	1

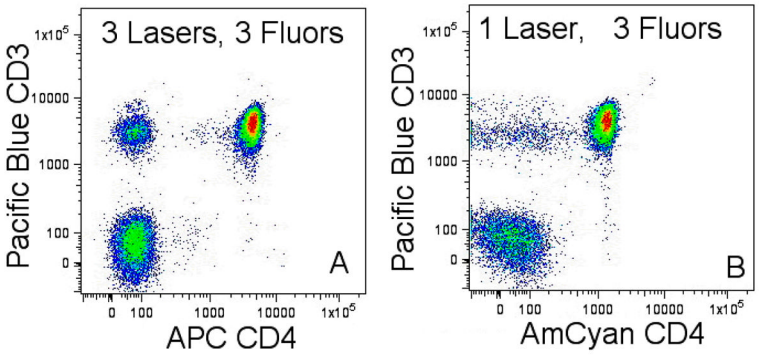

Figure 3. Reduced Spillover Using More Excitation Lines

Signal resolution for CD3 versus CD4 is much improved by excitation of 3 conjugated antibodies with three discreet light sources (left, 405nm, 532nm, 638nm for CD3-Pacific Blue, CD8-PE and CD4-APC) compared to one (right, 405nm for CD3-Pacific Blue, CD4-Amcyan and CD8-Pacific Orange).

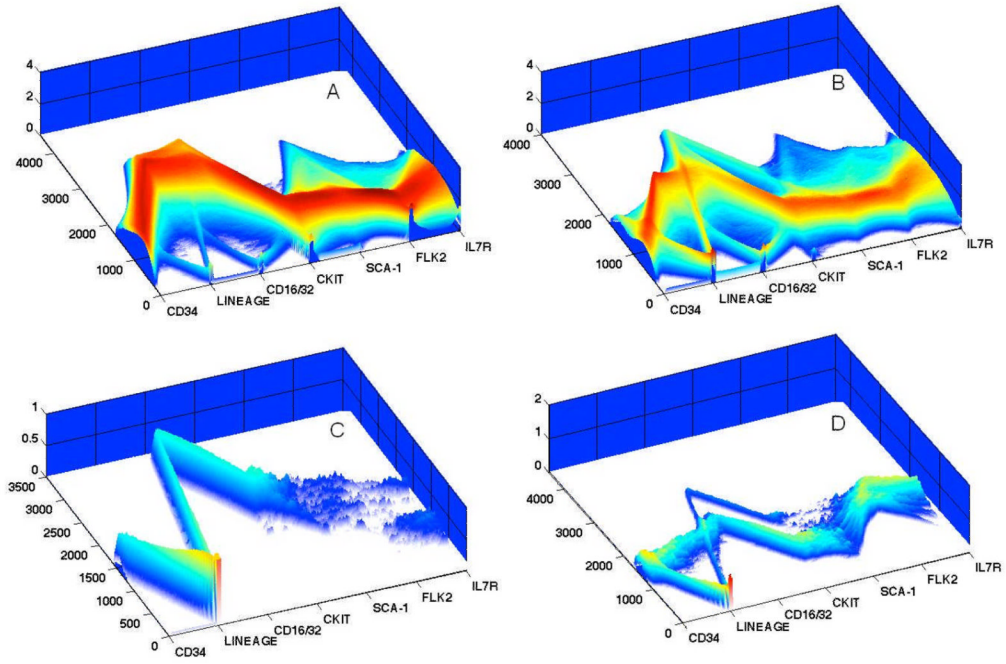

Figure 4. Parallel Coordinate Plots

Shown are four inter-related 3-dimensional parallel coordinate plots of a 1.5×10^6 event data file, gated initially on forward and side light scatter (Panel A), prior to omission of Lineage^{pos} cells, leaving remaining Lineage^{low} and Lineage^{neg} for further analysis (Panels B–D). Panel A represents total bone marrow cells; B are gated Lineage$^{low\text{-}neg}$ bone marrow cells; C are Lineage$^{low\text{-}neg}$ cKit+Sca-1+ cells; D are Lineage$^{low\text{-}neg}$ FLK2+ cells. Mouse bone marrow cells were stained with titered concentrations of CD34-FITC, CD16/32-Alexa700, cKit--APC, Sca-1-PECy5.5, FLK2-PE, IL-7-Pacific Blue and a murine lineage cocktail, consisting of biotinylated CD3, CD4, CD8, Mo2, Gr-1, Ter119, B220/CD45R and developed with streptavadin-PerCP. Panel A provides an overview of the relationships shown in 42 bivariate plots.

Parallel coordinates of immunofluorescent parameters are depicted on the x-axis, logarithmic fluorescent channel number intensity on y-axis, and the density of distributions on z-axis. To interpret the plots, one follows the relationship of antigenic co-expression across all parameters on the x-axis, the correlated fluorescent intensity of each parameter on the y-axis and the numbers of events depicted on the z-axis. For example, in looking across the x-axis of Panel C, as a result of cKit+Sca-1 gating, there is uniform expression of CD34, Lineage^{neg,} relatively high expression of CD16/32, robust expression of cKit and Sca-1 and bimodal expression of Flk2 and Il7R. There is a more complex relationship of the data in Panel D, which represents Lineage $^{low\text{-}neg}$ followed by selection of FLK2+ cells. Looking across parameters one sees uniform levels of CD34, two levels of Lineage $^{low\text{-}neg,}$ 2 two levels of CD16/32, negative and positive cKit and Sca-1 subpopulations, and two levels of IL7R expression.

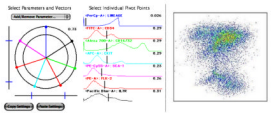

Figure 5. Polyvariate Plot

The mouse bone marrow sample described in Figure 4 was re-plotted as a 7 vector FlowJo Polyvariate plot. Vectors are arranged in a star pattern to provide identification of each monoclonal antibody -fluorochrome combination around a common central point. The arrangement of these fluorochrome conjugated antibodies is displayed by the colored lines displayed around a central point, and the histogram pivot range is displayed by colored histograms. The resulting Polyvariate Plot demonstrates the correlation of all seven parameters on one 2-dimensional plot, rather than numerous bivariate plots.

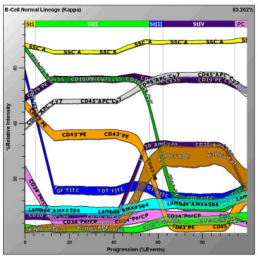

Figure 6. Probability State Model of Human B-Cell Maturation

Human bone marrow was stained with titered volumes of CD23-Pacific Blue, CD20-AmCyan, TdT-FITC, CD34-PerCP, CD43-PE, CD19-PeCy5.5, CD10-PECy7, Kappa – APC, CD45-APCCy7and Lambda- Alexa 594. Approximately 10,000 cells were analyzed and depicted in this Figure. The percentage of cells in each ‘state’ can be measured along the x-axis, and the level of antigen expression measured along the y-axis, where discreet colors are assigned to each parameter. B-cell precursors are seen to be down-regulating ‘early’ markers like CD34 and TdT and up-regulating more ‘mature’ antigens like CD20, CD23 and surface immunoglobulin light chain. These correlated variations are intuitively comprehensible since they are similar to the way a user might diagram the data. In contrast to the necessity of numerous conventional bivariate plots, Gemstone™ concisely depicts all these relationships in one plot.

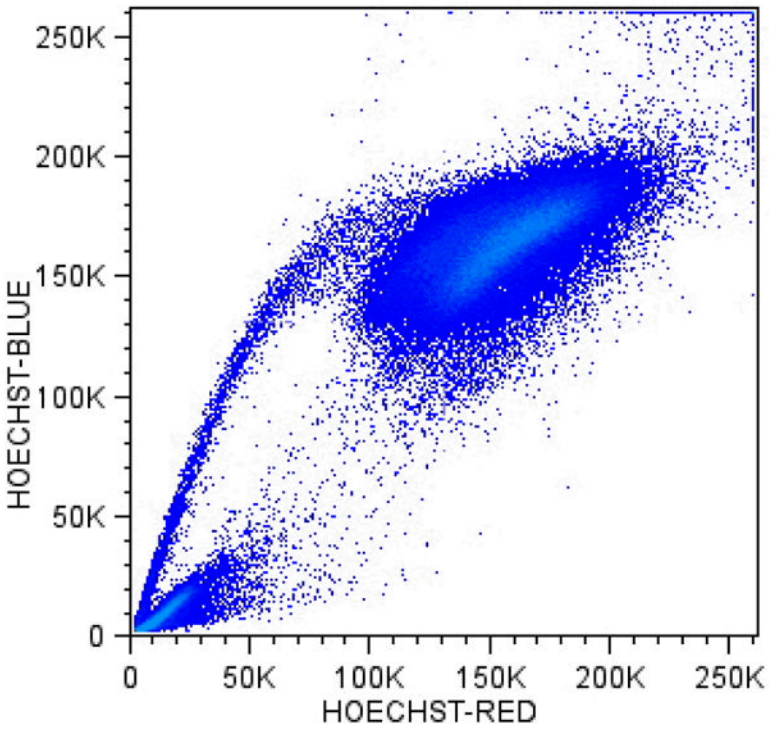

Figure 7. Side Population cells from Fallopian Tube

Cells isolated from benign human infundibular- fallopian tube biopsy freed with 1 hour incubation in collagenase were suspended in 1%Fcs DMEM and 5 ug/ml Hoechst 33342 for 1.5 hours at 37 C. Cells were re suspended in cold 1%FCS PBS and stained with four additional surface markers (not shown) for 15 minutes on ice and washed and re-suspended in 1%FCS PBS and stained with 7AAD and run on the author's multiple laser analyzer.

Table 1

Useful Fluorescent Probes and their Spectral Characteristics

Fluorochrome	Excitation Max(nm)	Excitation Lines(nm)	Emission Max(nm)	Emission Color
Propidium iodide	305, 540	350–360, 488	620	Yellow- Orange
Indo-1 Ca bound	330	350–360	405	Violet
Indo-1 Ca free	346	350–360	480	Blue
LIVE/DEAD blue	350	350–360	450	Blue
Hoechst 33342	352	350–360	455	Blue
AMCA-X	353	350–360	442	Blue
DAPI	359	350–360	461	Blue
Marina Blue	365	350–360	460	Blue
Alexa Fluor 350	346	350–360	442	Blue
Pacific Orange	400	405,407	551	Blue
Pacific Blue	404	405,407	456	Blue
BD Horizon V450	404	405,407	452	Blue
LIVE/DEAD violet	416	405,407	451	Blue
Alexa Fluor 405	405	405,407	420	Violet/Blue
ECFP	434	458,488	477	Blue
AmCyan	458	405,407	489	Blue
EGFP	489	458,488	508	Cyan
Alexa Fluor 430	430	405,407	540	Green
CFSE	490	488	518	Green
PKH2 & PKH67	490	488	504	Green
LIVE/DEAD green	495	488	520	Green
Alexa Fluor 488	495	488	519	Green
FITC	494	488	519	Green
Rhodamine 123	507	488	529	Yellow-Green
Ethidium monoazide	510	488	600	Yellow- Orange
EYFP	514	488,532	527	Yellow-Green
Alexa Fluor 532	531	532	554	Yellow-Green
PKH26	551	488,532	567	Yellow-Green
DsRed	558	568	583	Yellow
PE	496,546	488,532	578	Yellow
PE-Texas Red	496,546	488,532	615	Yellow- Orange
HcRed	588	532,568,590,594	618	Yellow- Orange
Alexa Fluor 594	590	594	617	Yellow- Orange
LIVE/DEAD red	595	488	615	Yellow- Orange
Texas Red	595	595	615	Yellow- Orange
7-AAD	550	488,532,594	660	Red
DRAQ5	646	633	681	Red

Fluorochrome	Excitation Max(nm)	Excitation Lines(nm)	Emission Max(nm)	Emission Color
APC	650	595,633,635,647	660	Red
Alexa Fluor 647	650	595,633,635,647	668	Red
PE-Cy5	496,546	488,532	667	Red
Cy5	640	633,635	670	Red
PerCP	482	488,532	678	Red
Alexa Fluor 660	663	647	690	Red
LIVE/DEAD far red	650	633,635	665	Red
APC-Cy5.5	650	633,635	694	Red
PerCP-Cy5.5	482	488,532	695	Red
PE-Cy7	496,546	488,532	785	InfraRed
APC-Cy7	650	595,633,635,647	785	InfraRed
APC-Alexa Flour 750	650	595,633,635,647	775	InfraRed
HiLyte 750, no tandem	753	785	778	InfraRed
IRDye 800CW	774	785	789	InfraRed
Q-dots/eFluor/AxiCad	various	350–360, 407	various	Various

Table 2

Antigen	Other Names	Differentiated Cell Expression	Stem/Progenitor Expression
CD34	8G12, 581, QBEnd10	endothelial	HSC
CD105	Endoglin	endothelial, macrophage/monocyte	mesenchymal, with CD73+, CD16+, CD90+ CD29+ CD34−, CD45−, Lin−
CD90	Thy-1	murine pan T, thymocyte, fibroblast	murine hematopoietic, neural
CD117	c-kit, steel, stem cell factor	breast epithelial, renal tubule, melanocytes	myeloid, HSC
CD133	AC133, Prominin-1	endothelium, epithelial	HSC, endothelial, and neural epithelial
CD135	FMS-like kinase-3 (FLT3) or STK-1, or Flk-2	macrophage/monocytes	human marrow CD34+ & dendritic precursors, murine short-term -HSC
CD150	SLAMf1; used with CD244 and CD48	T,B, dendritic, endothelial	distinguishes HSC from multipotent and B cell progenitors
SCA-1	stem cell antigen; when used with cKit and Lin- the combination is ‘ LKS’		HSC